investigated the numbers of intracellular *Mtb*, since *Mtb* was reported previously to grow rapidly inside macrophages (van der Wel *et al.*, 2007). The numbers of intracellular *Mtb* increased after a five day culture of the osteoclasts. Notably, *Mtb* grew better in multinuclear osteoclasts than in mononuclear cells; there were four times as many intracellular *Mtb* in the mOCs than in pMCs on day 5 of culture (Fig. 1b). These results suggest that living *Mtb* has a greater ability to expand intracellularly following the infection of multinuclear osteoclasts than mononuclear osteoclast precursors.

We next evaluated the intracellular localization of the living *Mtb* in multinuclear osteoclasts using electron microscopic analysis, because the intracellular localization of *Mtb* inside the macrophage has been a matter of debate in recent years (Welin & Lerm, 2012). *Mtb* has the ability to grow in macrophages by arresting the normal process of phagosome maturation. As part of their strategy for intracellular survival, mycobacteria prevent the maturation of the phagosomes, in which they reside inside macrophages. Notably, we observed no significant phagosome membrane around the intracellular *Mtb* in our study (Fig. 1c and d). These data demonstrated that *Mtb* escapes from osteoclastic phagosomes, whereas the bacteria were arrested in phagosomes of macrophages. Escape from phagosomes could drive the more rapid expansion of *Mtb* in osteoclasts. During our electron microscopic analysis, we did not observed any significant phagosome membrane formation around intracellular *Mtb* (Fig. 1d). It is well known that *Mtb* survives inside macrophage phagosomes, whose normal maturation process is arrested by the bacteria (Fratti *et al.*, 2001; Pethe *et al.*, 2004). Thus, *Mtb* interrupts the acidification of endosomes, followed by the fusion of acidic endosomes and lysosomes. As a result, the immature endosomes maintain a high pH (> 6.4) (Pethe *et al.*, 2004), which leads to a failure of the cells to supply hydrolytic enzymes and antimicrobial peptides (Rohde *et al.*, 2007a, b). Our previous report also provided support for the hypothesis that *Mtb* resides inside endosomes to form multilocal necrotic lesions in the lung, liver, and spleen tissues (Yamada *et al.*, 2002), and that phagolysosomal fusion incorporating many tubercle bacilli is prominent (Yamada *et al.*, 2001). In contrast, our current results demonstrated that there are *Mtb*-containing phagosomes/endosomes inside the multinuclear osteoclasts (see Fig. 1d). The fact that *Mtb* escapes from the endosome/phagosome might be due to the endosomal acidification; osteoclasts expressed higher amounts of acid-producing vacuolar type H^+-ATPase (V-ATPase) for osteolysis. Similar bacterial evacuation from the endosomes is observed for other mycobacteria species. An acid-fast bacillus, *Mycobacterium marinum*, which causes a systemic tuberculosis-like disease in its natural hosts, such as fish and frogs, was reported to escape from phagosomes (Stamm *et al.*, 2003). In addition, intracellular pathogens, including *Listeria monocytogenes*, *Shigella flexneri*, and *Rickettsia rickettsii* (Goldberg, 2001) also share the ability to enter the host cell cytoplasm, induce actin polymerization, and use actin-based motility to spread between host cells during intracellular infection.

Living *Mtb* have the ability to facilitate osteolytic response by multinuclear osteoclasts rather than proinflammatory responses

We investigated whether proinflammatory responses were induced by intracellular *Mtb*-infected multinuclear osteoclasts. To assess the productivity of proinflammatory cytokines during osteoclastogenesis in response to living *Mtb*, the production of proinflammatory cytokines (TNF-α and IL-1β) and proinflammatory chemokines (MCP-1/CCL2 and MIP-1α/CCL3) in response to intracellular *Mtb* infection by mOCs were measured (Fig. 2a and b). We found that *Mtb*-infected mOCs lost the ability to produce proinflammatory cytokines (TNF-α and IL-1β) and proinflammatory chemokines (MCP-1/CCL2 and MIP-1α/CCL3), whereas *Mtb*-infected pMCs retained the ability to produce these proinflammatory factors. Surprisingly, the production level of another proinflammatory cytokine IL-6 decreased by half, suggesting that the basal level of IL-6 production of pMCs was dampened by the early phase of *Mtb* infection. Notably, we detected no IFN-γ production during osteoclastogenesis (data not shown), although IFN-γ is involved in Th_1-mediated immune response and is followed by the formation of granulomatous caseous necrosis observed around destroyed bone tissue (Schluger & Rom, 1998). The data demonstrate that the production patterns of proinflammatory cytokines in inflammatory sites with bone destruction in tuberculosis lesions might be different from those of other inflammatory conditions, such as rheumatoid arthritis.

In addition, the enzymatic activity of tartrate-resistant acid phosphatase (TRAP), which is the principal osteolytic enzyme secreted in the culture supernatant, was measured (Fig. 2c). In pMCs, elevated TRAP activity was observed in unstimulated pMCs, although *Mtb*-infected pMCs showed decreased TRAP production. This was in contrast to several previous reports suggesting that TNF-α is an enhancer of inflammatory osteolysis in bone destructive lesions (Abu-Amer *et al.*, 1997; Lam *et al.*, 2002). As reported previously, bacterial products, LPS (a ligand for TLR4) and Pam_3CSK_4 (a TLR2 ligand), has the ability to promote TRAP secretion by pMCs (Fig. 2d), indicating that osteoclastogenesis is accelerated not only by TNF-α but also by TLR-ligands. However, intracellular *Mtb* infection in mOCs sustained, whereas TLR-ligands obstructed, the TRAP secretion (Fig. 2c and d). These findings are in agreement with previous reports that the ligands for TLR4 inhibit osteoclast differentiation (Itoh *et al.*, 2003; Chang *et al.*, 2007).

In contrast to TRAP activity, the transcriptional level of another osteolytic enzyme, cathepsin K, was enhanced by pMCs in response to *Mtb* (Fig. 2e). Thus, intracellular infection of *Mtb* resulted in a different osteolytic response than typical microbial responses via TLR-mediated signals. We confirmed that the expression levels of TLR2 and TLR4 were not significantly changed during osteoclastogenesis (data not shown). Inflammatory activation signals in response to intracellular *Mtb*, which seems to be independent of the TLR-mediated pathways, could interrupt the osteoclast development.

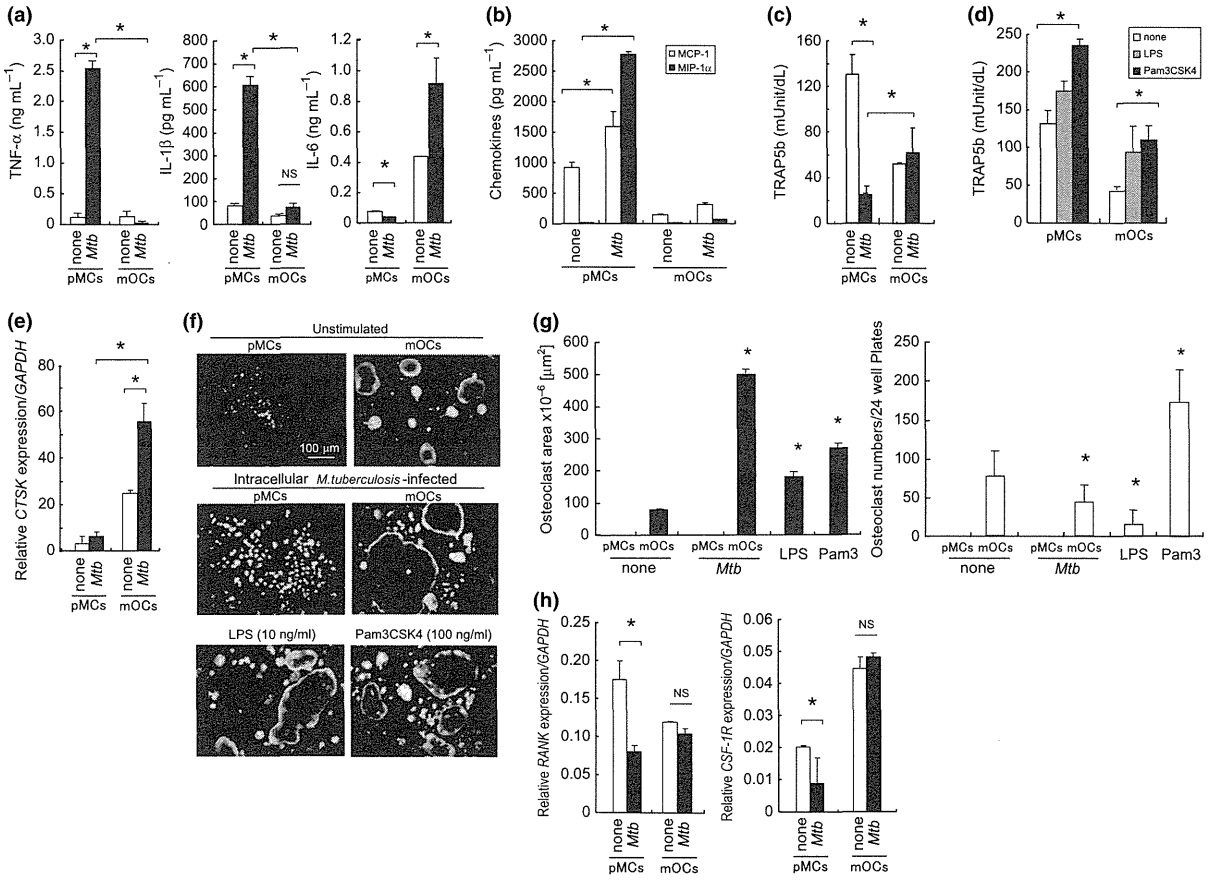

Fig. 2 The production of pro-inflammatory cytokines, chemokines and an osteoclast-specific enzyme by pre-osteoclasts and multinuclear osteoclasts after *Mtb* infection. (a,b) The production of (a) the proinflammatory cytokines TNF-α, IL-1β and IL-6, and (b) the proinflammatory chemokines MCP-1/CCL2 and MIP-1α/CCL3 for 24 h after *Mtb* infection, were measured by an ELISA. The data show the means ± SD (n = 6). (c,d) The levels of Trap5b in pMCs and mOCs stimulated with *Mtb* (10^5 CFU mL^{-1}), LPS (10 ng mL^{-1}) and Pam_3CSK_4 (100 ng mL^{-1}) were measured by an ELISA. The data show the means ± SD (n = 6). (e) The relative expression levels of an osteolytic enzyme, cthepsin K (*CTSK*), produced by pMCs and mOCs, stimulated with *Mtb*, were measured by real-time Q-PCR. The data show the means ± SD (n = 4). (f,g) In (f) the area and the numbers of osteoclasts after *Mtb* (10^5 CFU mL^{-1}), LPS (10 ng mL^{-1}), and Pam_3CSK_4 (100 ng mL^{-1}) stimulation were visualized by immunohistochemical staining using an anti-cathepsin K antibody conjugated with Alexa594 (red). F-actin and nuclei were counterstained by phalloidin–AlexaFluor 488 (green) and hoechst33258 (blue), respectively. Magnification ×400. (g) Histograms of the area distribution of multinuclear osteoclasts delimited with phalloidin and of the number of multinuclear osteoclasts in (f). The data are presented as the means ± SD (n = 3). (h) The relative expression levels of the RANKL receptor (*RANK*) and M-CSF receptor (*CSF1R*) by pMCs and mOCs stimulated with *Mtb* were measured by real-time Q-PCR. The data show the means ± SD (n = 4).

We next investigated whether *Mtb* infection exerts a facilitatory effect on osteoclast formation, because bacterial products are reported to utilize two different pathways via TLR4 in both survival and cytokine production of osteoclasts (Itoh *et al.*, 2003). Compared with mOCs, *Mtb* infection by pMCs did not facilitate the formation of multinuclear osteoclasts (Fig. 2f and g). Stimulation of pMCs by Pam_3CSK_4 also resulted in formation of large numbers of large multinuclear osteoclasts. In contrast, in response to LPS, pMCs increased the number of osteoclasts with diminished osteoclast area. The result indicates that LPS facilitates the osteoclast formation but not osteoclastic activation directly via TLR4. Notably, we found that the osteoclast area increased in response to *Mtb*, although the osteoclast numbers were decreased by *Mtb* stimulation (Fig. 2g), indicating that intracellular *Mtb* infection facilitates osteoclast formation but abrogates typical osteoclastic activation. Therefore, intracellular *Mtb* infection induces irregular osteoclastogenesis by shifting the properties of osteoclasts from osteolytic to inflammation.

We then investigated whether the changes in the properties of *Mtb*-infected osteoclasts were due to the dysfunction of the RANK-RANKL axis, which is the principal osteoclastic regulator. *Mtb*-infected pMCs exhibited decreased expression levels of *RANK* and *c-fms*, which encodes CSF-1R, the receptor for M-CSF (Fig. 2h). These data indicated that *Mtb*-infected pMCs lost their ability to differentiate into osteoclasts in response to osteoclastogenic

growth factors M-CSF and RANKL as a result of downregulation of their receptors on osteoclasts. Consequently, *Mtb* infection by pMCs leads to dysfunction in the physiological osteoclastogenesis process and facilitates the inflammatory osteoclastic activation. However, it is still unknown why the development of osteoclasts from the precursor cells was inhibited by intracellular *Mtb* infection but not by the TLR-ligands. Various reports have suggested that there are differences in the biological responses induced by TLRs and RANK, although both TLRs and RANK share a common downstream signaling molecule, TRAF-6 (Mansell *et al.*, 2004; Takeda & Akira, 2005). One possible reason for this is that the early secreted antigen, ESAT-6, facilitates the recognition of *Mtb* in cooperation with TLR2 in macrophages (Pathak *et al.*, 2007).

Specific expression profiles of chemokine ligands and their counterpart receptors are induced by *Mtb*-infected osteoclasts

Several reports suggested the participation of chemokines during physiological osteoclastogenesis (Oba *et al.*, 2005; Menu *et al.*, 2006; Hoshino *et al.*, 2009, 2010), which is induced by the combination of M-CSF and RANKL. The fact that intracellular *Mtb* infection disturbs the physiological osteoclastogenesis prompted us to investigate whether intracellular *Mtb* infection could disrupt the chemokine profiles. Therefore, we compared the chemokine expression profiles in response to intracellular *Mtb* infection. We noted that various chemokine ligands are selectively produced by osteoclasts at mRNA transcription level (Supporting Information, Fig. S1). Among these ligands, *CCL5* (also called RANTES) was highly upregulated during osteoclastogenesis (Fig. 3a), consistent with the chemokine expression profile in murine osteoclastogenesis (Hoshino *et al.*, 2010). In addition, pMC expressed small amounts of chemokines, namely, *CCL17*, *CCL20*, *CCL22*, *CCL24*, and *CCL25* (Fig. 3a). However, mature mOCs failed to produce these proinflammatory chemokines in response to *Mtb* infection.

To confirm that the immune response to virulent *Mtb* strains is different from the response to non-virulent strains, we measured the transcription of the chemokines by pMCs and mOCs in response to an avirulent *Mtb* strain (H37Ra) and a BCG-Tokyo strain. Both the avirulent H37Ra strain

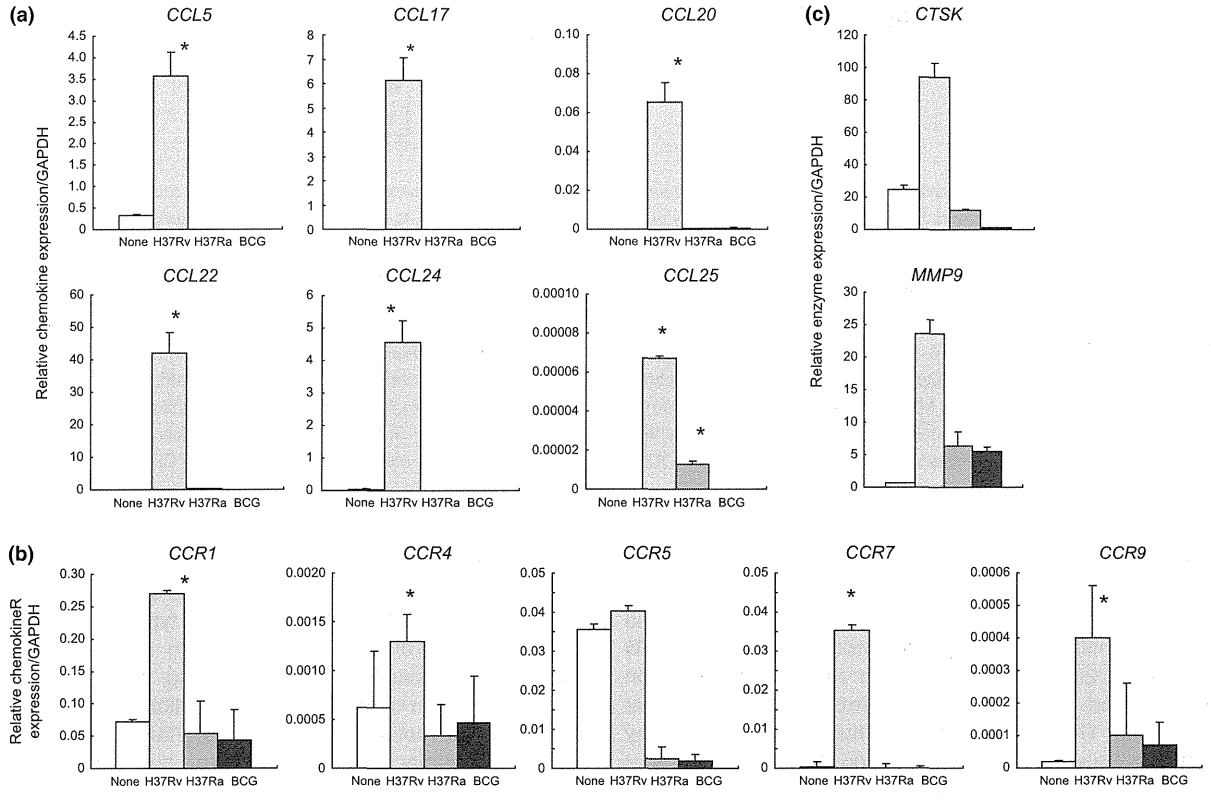

Fig. 3 The expression levels of chemokine ligands and their receptors by osteoclasts after *Mtb* infection. (a–c) The relative expression levels of CC-chemokine ligands by pMCs (a), and CC-chemokine receptors by mOCs (b), and osteolytic enzymes cathepsin K (*CTSK*) bone-specific matrix metalloproteinase (*MMP9*) (c), stimulated with a virulent strain *Mtb* H37Rv (*c.* 6.0×10^5 CFU mL^{-1}), an avirulent strain *Mtb* H37Ra (*c.* 8.7×10^5 CFU mL^{-1}) or a BCG strain (*c.* 3.4×10^5 CFU mL^{-1}) were measured by real-time Q-PCR. *Statistically significant differences ($P < 0.05$); N.D., not detected.

and the BCG strain had a decreased ability to induce the production of the chemokine ligands by osteoclasts (Fig. 3a).

We next investigated the expression profile of C-C chemokine receptors during human osteoclastogenesis. In previous murine experiments we reported that the selective upregulation of two chemokine receptors, CCR1 and CCR5, which are required for osteolytic enzyme production (Hoshino *et al.*, 2009), occurred with the downregulation of other chemokine receptors during murine osteoclastogenesis (Hoshino *et al.*, 2009, 2010). Among the chemokine receptors evaluated, CCR1 and CCR5 were both upregulated during human osteoclastogenesis (Fig. 3b). Besides the virulent *Mtb* strain, H37Rv infection also upregulated the expression of *CCR1*, *CCR7*, and *CCR9*, whereas there was diminished expression of *CCR2, CCR3, CCR6*, and CX_3CR1 (Fig. 3b, Fig. S2). The avirulent *Mtb* strain (H37Ra) had sustained expression of *CCR1* during osteoclastogenesis, whereas the expression of other chemokine receptors decreased. The osteolytic enzyme cathepsin K (*CTSK*) is also expressed only following infection with the virulent *Mtb* strain (Fig. 3c). An enzyme matrix metalloproteinase-9 (*MMP9*), which was secreted mainly by epithelial cells surrounding the growing granuloma and promoted the recruitment of new macrophages to the granuloma (Volkman *et al.*, 2010), was also expressed with the virulent *Mtb* stimulation. As CCR1 is the most abundant chemokine receptor during osteoclastogenesis, we next investigated the expression of CCR1 and CCR5 in multinuclear cells in a granuloma from a tissue section of the *Mtb*-infected patient (Fig. 4), and the results suggested that the expression of chemokine receptors plays a role during multinuclear cell formation in the pathological condition. Therefore, intracellular *Mtb* infection induces the evacuation of *Mtb* into the cytosol, which leads to irregular osteoclastogenesis as a result of the dysregulation of chemokines, chemokine receptors, and osteoclastic molecules, and finally results in a shift in the properties of osteoclasts from osteolytic to inflammatory.

Infection of osteoclasts with *Mtb* produces specific chemokines

To further investigate whether these chemokine responses are specific for *Mtb* infection, we measured and compared the production of these chemokines after *Mtb* infection, and LPS stimulation by pMCs and mOCs (Fig. 5). As previously mentioned, inflammatory chemokines CCL2/MCP-1 and CCL3/MIP-1α are produced in limited numbers by *Mtb*-infected pMCs (see Fig. 1b). Instead, abundant production of several chemokines by mOCs was observed: (1) a common proinflammatory response to both LPS and intracellular *Mtb* infection, (2) a *Mycobacteria*-specific chemokine response, and (3) an intracellular virulent *Mtb* infection -specific chemokine response. The first group of chemokines, CCL5, CCL24, and CCL17, are commonly produced in response to both LPS and intracellular *Mtb* stimulation (Fig. 5a–c), suggesting that the activation of the CCR5-CCL5, CCR4-CCL17, and CCR3-CCL24 axes is a common infectious response of multinuclear osteoclasts. Notably, the CCL17 production was limited to mOCs (Fig. 5c), implying that the activation of the CCR4-CCL17 axis reflects abnormal osteoclast activation. The second group of chemokines, including CCL22, was enhanced by virulent *Mtb* H37Rv infection, as well as avirulent H37Ra infection (Fig. 5d). CCL22 was physiologically produced by unstimulated mOCs, and its production was pathologically enhanced by pMCs in response to both LPS and *Mtb* stimulation, indicating that the aberrant production of CCL22 by pMCs might be a facilitator for the abnormal osteoclastic activation. Interestingly, the production of the third group of chemokines, CCL20 and CCL25, which was enhanced by virulent *Mtb* infection, was observed only by mOCs (Figs. 5e and f). The data suggested that CCL20 and CCL25 might play pivotal roles in the osteolytic response of virulent *Mtb*-infected bone tissue. These findings suggest that the pivotal role of chemokines in pathological osteoclastogenesis was via the combined production of osteoclast-specific chemokines, such as CCL17, and *Mtb*-specific chemokines,

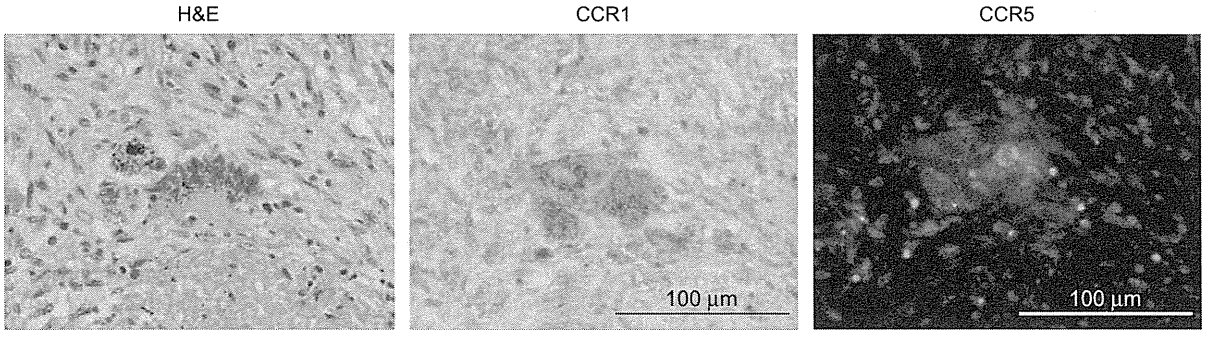

Fig. 4 Expression of chemokine receptors CCR1 and CCR5 in *Mtb*-infected multinuclear granuloma in a tuberculosis patient. (Center panel) Immunohistochemical staining of chemokine receptor CCR1 visualized by an anti-human CCR1 antibody and followed by DAB chromogen. Nuclei were counterstained using hematoxylin. Magnification ×400. (Right panel) Immunohistochemical staining of chemokine receptor CCR5 visualized by an anti-human CCR5 antibody conjugated with phycoerythrin (red). Nuclei were counterstained by Cyto13® green fluorescent dye in green. Magnification ×400. (Left panel) H&E stain of counterpart section. Scale bar: 100 μm.

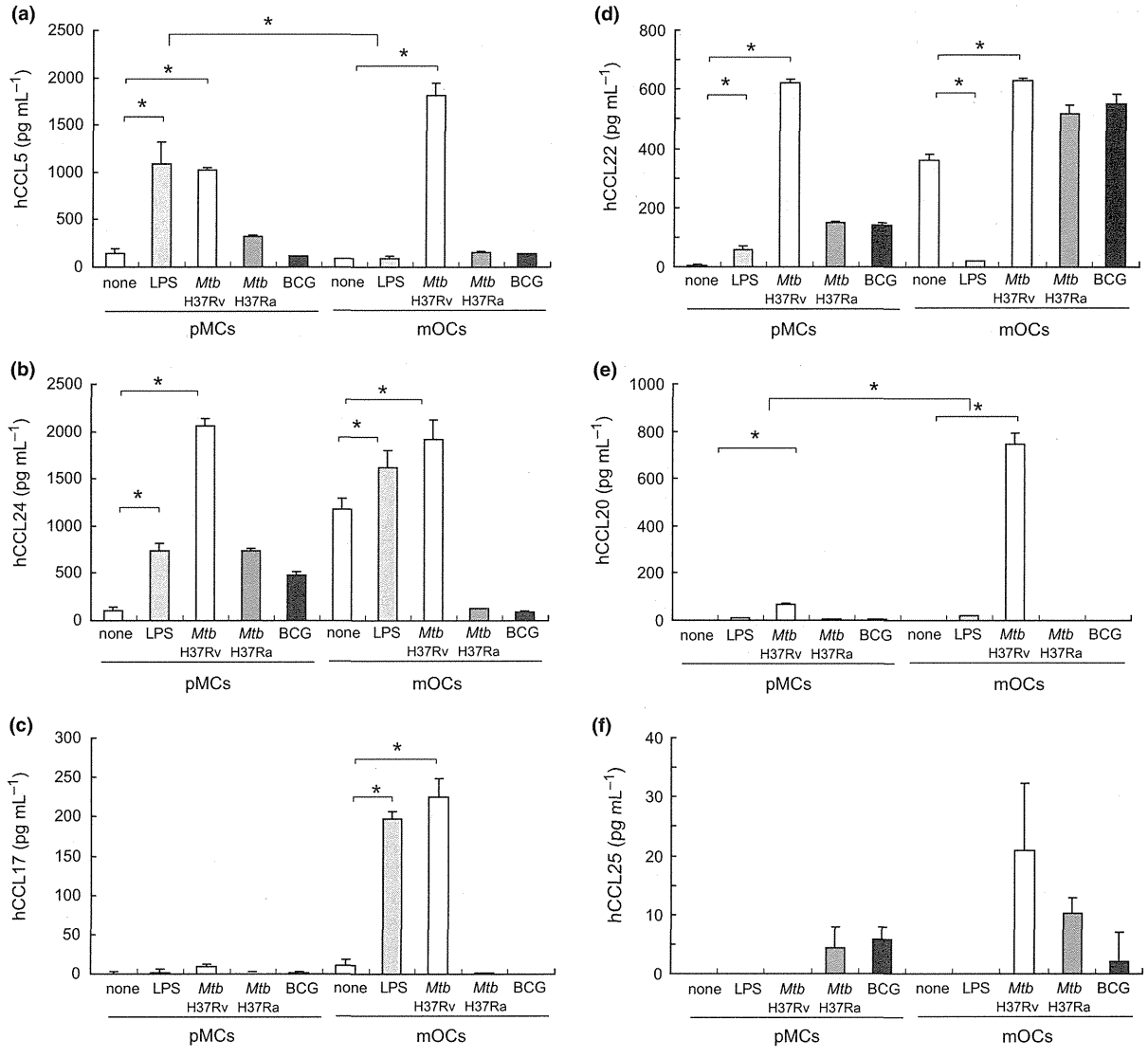

Fig. 5 The production of several chemokines by multinuclear osteoclasts stimulated with *Mtb*. The production of chemokines CCL5 (a), CCL24 (b), CCL17 (c), CCL22 (d), CCL20 (e), and CCL25 (f) in pMCs and mOCs stimulated with the bacterial product LPS (100 ng mL^{-1}), virulent *Mtb* H37Rv strain (*c.* 6.0 × 10^5 CFU mL^{-1}), avirulent *Mtb* H37Ra strain (*c.* 8.7 × 10^5 CFU mL^{-1}), and BCG strain (*c.* 3.4 × 10^5 CFU mL^{-1}) were measured by an ELISA. The data are presented as the means ± SE of duplicate samples (n = 3). ND, not detected.

including CCL20, CCL22, and CCL25, in response to evacuated *Mtb* in the cytosol.

The findings of the present study demonstrate that the intracellular infection of multinuclear osteoclasts by *Mtb* failed to induce the secretion of typical proinflammatory cytokines and proinflammatory chemokines, such as TNF-α, IL-1β, CCL2/MCP-1 or CCL3/MIP-1α (Fig. 2), but resulted in the selective expression of osteoclast-specific chemokines and their receptors (Fig. 3). However, the combination of chemokine ligands and their receptors do not have a one-to-one correspondence; the induction ratio of chemokine receptors after virulent *Mtb* infection revealed that *Mtb* infection activates a very limited number of chemokine ligands, namely *CCL5, CCL17, CCL19, CCL20, CCL22, CCL24*, and *CCL25* (Fig. 3a, Fig. S1), which was followed by the induction of their corresponding chemokine receptors, such as *CCR1*, *CCR4*, *CCR5*, *CCR7*, and *CCR9* (see Fig. 3b). Thus, these chemokine axes could be an important chemokine-mediated response induced by intracellular *Mtb* infection. Among them, the chemokine axes of CCR1/CCR5-CCL5, CCR4-CCL17/CCL22, and CCR9-CCL25 could play roles in the chemokine-mediated response to intracellular *Mtb* infection. In support of this, both CCR1 and CCR5 were highly expressed in multinuclear granuloma cells by a *Mtb*-infected patient (Fig. 4). In addition, several clinical papers indicated the involvement of the chemokine

system in intracellular *Mtb* infection; CCR7 is related to the progression of several inflammatory bone diseases, such as rheumatoid arthritis (Bugatti *et al.*, 2005; Pickens *et al.*, 2011) and a murine model of tuberculosis (Kahnert *et al.*, 2007; Khader *et al.*, 2009). The involvement of the CCR9–CCL25 axis in rheumatoid arthritis was also reported (Endres *et al.*, 2010; Schmutz *et al.*, 2010). CCL22 and its receptor, CCR4, are highly expressed in the lungs, especially in tuberculous lungs (Volpe *et al.*, 2006; Okamoto *et al.*, 2007; Wu *et al.*, 2010), and it has also been reported to be produced by human osteoclasts in response to foreign substances, such as titanium particles (Cadosch *et al.*, 2010). These data provide new aspects of how CCR4 switches its ligands, CCL17 and CCL22. The mechanism leading to the switch in the specific chemokine axes could play a pivotal role during pathological osteoclastogenesis via virulent *Mtb* infection. Further investigations will be needed to clarify the osteolytic mechanism of skeletal tuberculosis.

In conclusion, we have characterized the pathological activation of osteoclasts in response to intracellular *Mtb* infection. Our data indicate that the inflammatory osteoclastogenesis by *Mtb* infection is facilitated not only by proinflammatory chemokines such as TNF-α, and by the activation of the RANK-RANKL pathways, but also by the production of specific chemokines in response to intracellular *Mtb* infection. Notably, we did not detect any TNF-α production by *Mtb*-infected multinuclear osteoclasts (see Fig. 2a). TNF-α is responsible for granuloma formation and maintenance, and the deficiency of TNF-α resulted in hypersusceptibility to tuberculosis (Ramakrishnan, 2012). Thus, the unresponsiveness of TNF-α might cause the defective immune response during the early stages of *Mtb* infection. Although early infection of macrophages might be predicted to promote initial host immunity, *Mtb* impairs antigen presentation and an effective adaptive immune response. Furthermore, we found that the intracellular *Mtb* inside multinuclear osteoclasts escaped from the endosome/phagosome, and led to dysregulation of osteoclast activation. Aberrant production of chemokines is due to the evacuation of *Mtb* from the endosome/phagosome, which accomplishes to avoid acidification. Evacuated *Mtb* in cytosol might lead to dysregulation of cytokines and chemokines, which promotes atypical osteoclast activation, and finally causes pathological bone destruction in the bone tissue. Consequently, our data suggest that the source of *Mtb*-activated osteoclasts in spinal tuberculosis could be derived from tissue-resident multinuclear osteoclasts that were unexpectedly activated in response to *Mtb* infection. Our findings provide novel information about an atypical type of inflammation that is independent of proinflammatory cytokine production due, in the case of osteoclast activation to spinal tuberculosis.

The present observations provide further evidence that the chemokine/chemokine receptor axes in bone metabolism play pathological roles, including the functional differentiation of osteoclasts following intracellular infection. Our current findings emphasize the relevance of the chemokine axes as exacerbating factors for bone destruction diseases. The dysregulation of cytokines and chemokines appears to play a pivotal role in the abnormal differentiation of macrophage-lineage cells via reprogramming of the inflammatory responses involved in pathological bone metabolism. Further studies are needed to clarify the mechanism of destruction following intracellular infections with pathogens.

Acknowledgements

The author is grateful to Prof. Yoshichika Arakawa and Dr. Keiko Yamada (Dept. Bacteriology/Drug Resistance and Pathogenesis, Nagoya University Graduate School of Medicine) for kindly providing a vaccine strain of *Mycobacterium bovis* strain BCG-Tokyo/Nagoya. This work was mainly supported by a KAKENHI Grant-in-aid for young scientists B (2010–2011, #22790359), and by a research fellowship from the Japan Society for the Promotion of Science for Young Scientists (2007–2009) to A.H.

Authors' contributions

A.H. and S.H. performed the experiments and analyzed the data for H.Y., Sa.M., and Y.M.; H.Y. and Sa.M. provided the equipment, the Bio Safety Level-3 facility for Mtb experiments, and virulent Mtb strain H37Rv; Sh.M. and M.T. provided the paraffin-embedded tissue section of tuberculosis patients; A.H., Y.M., and K.Y. designed the research; A.H. wrote the paper. Contact authors: Yoshinobu Manome (manome@jikei.ac.jp), Akiyoshi Hoshino (hoshinoa@nih.go.jp; hoshino.akiyoshi@med.nagoya-u.ac.jp).

References

Abu-Amer Y, Ross FP, Edwards J & Teitelbaum SL (1997) Lipopolysaccharide-stimulated osteoclastogenesis is mediated by tumor necrosis factor via its P55 receptor. *J Clin Invest* 100: 1557–1565.

Binder NB, Niederreiter B, Hoffmann O, Stange R, Pap T, Stulnig TM, Mack M, Erben RG, Smolen JS & Redlich K (2009) Estrogen-dependent and C-C chemokine receptor-2-dependent pathways determine osteoclast behavior in osteoporosis. *Nat Med* 15: 417–424.

Boyle WJ, Simonet WS & Lacey DL (2003) Osteoclast differentiation and activation. *Nature* 423: 337–342.

Bugatti S, Caporali R, Manzo A, Vitolo B, Pitzalis C & Montecucco C (2005) Involvement of subchondral bone marrow in rheumatoid arthritis: lymphoid neogenesis and *in situ* relationship to subchondral bone marrow osteoclast recruitment. *Arthritis Rheum* 52: 3448–3459.

Cadosch D, Gautschi OP, Chan E, Simmen HP & Filgueira L (2010) Titanium induced production of chemokines CCL17/TARC and CCL22/MDC in human osteoclasts and osteoblasts. *J Biomed Mater Res A* 92: 475–483.

Chang EJ, Kim HJ, Ha J *et al.* (2007) Hyaluronan inhibits osteoclast differentiation via Toll-like receptor 4. *J Cell Sci* 120: 166–176.

Choi SJ, Cruz JC, Craig F, Chung H, Devlin RD, Roodman GD & Alsina M (2000) Macrophage inflammatory protein 1-alpha is a potential osteoclast stimulatory factor in multiple myeloma. *Blood* 96: 671–675.

Dairaghi DJ, Oyajobi BO, Gupta A *et al.* (2012) CCR1 blockade reduces tumor burden and osteolysis *in vivo* in a mouse model of myeloma bone disease. *Blood* 120: 1449–1457.

Endres M, Andreas K, Kalwitz G, Freymann U, Neumann K, Ringe J, Sittinger M, Haupl T & Kaps C (2010) Chemokine profile of synovial fluid from normal, osteoarthritis and rheumatoid arthritis patients: CCL25, CXCL10 and XCL1 recruit human subchondral mesenchymal progenitor cells. *Osteoarthritis Cartilage* 18: 1458–1466.

Fratti RA, Backer JM, Gruenberg J, Corvera S & Deretic V (2001) Role of phosphatidylinositol 3-kinase and Rab5 effectors in phagosomal biogenesis and mycobacterial phagosome maturation arrest. *J Cell Biol* 154: 631–644.

Goldberg MB (2001) Actin-based motility of intracellular microbial pathogens. *Microbiol Mol Biol Rev* 65: 595–626, table of contents.

Han JH, Choi SJ, Kurihara N, Koide M, Oba Y & Roodman GD (2001) Macrophage inflammatory protein-1alpha is an osteoclastogenic factor in myeloma that is independent of receptor activator of nuclear factor kappaB ligand. *Blood* 97: 3349–3353.

Haringman JJ, Smeets TJ, Reinders-Blankert P & Tak PP (2006) Chemokine and chemokine receptor expression in paired peripheral blood mononuclear cells and synovial tissue of patients with rheumatoid arthritis, osteoarthritis, and reactive arthritis. *Ann Rheum Dis* 65: 294–300.

Haynes DR (2004) Bone lysis and inflammation. *Inflamm Res* 53: 596–600.

Hoshino A, Ueha S, Imai T, Kirino T, Matsushima K & Yamamoto K (2009) Deficiency of chemokine receptors CCR1, CCR5 and CX3CR1 causes defective osteoclast differentiation and defective bone remodeling. *Bone* 44(suppl 2): S215.

Hoshino A, Iimura T, Ueha S *et al.* (2010) Deficiency of chemokine receptor CCR1 causes osteopenia due to impaired functions of osteoclasts and osteoblasts. *J Biol Chem* 285: 28826–28837.

Hoshino A, Ueha S, Hanada S, Imai T, Ito M, Yamamoto K, Matsushima K, Yamaguchi A & Iimura T (2013) Roles of chemokine receptor CX3CR1 in maintaining murine bone homeostasis through the regulation of both osteoblasts and osteoclasts. *J Cell Sci* 126: 1032–1045.

Itoh K, Udagawa N, Kobayashi K, Suda K, Li X, Takami M, Okahashi N, Nishihara T & Takahashi N (2003) Lipopolysaccharide promotes the survival of osteoclasts via Toll-like receptor 4, but cytokine production of osteoclasts in response to lipopolysaccharide is different from that of macrophages. *J Immunol* 170: 3688–3695.

Ji JD, Park-Min KH, Shen Z, Fajardo RJ, Goldring SR, McHugh KP & Ivashkiv LB (2009) Inhibition of RANK expression and osteoclastogenesis by TLRs and IFN-gamma in human osteoclast precursors. *J Immunol* 183: 7223–7233.

Jiang Y, Mehta CK, Hsu TY & Alsulaimani FF (2002) Bacteria induce osteoclastogenesis via an osteoblast-independent pathway. *Infect Immun* 70: 3143–3148.

Kahnert A, Hopken UE, Stein M, Bandermann S, Lipp M & Kaufmann SH (2007) *Mycobacterium tuberculosis* triggers formation of lymphoid structure in murine lungs. *J Infect Dis* 195: 46–54.

Khader SA, Rangel-Moreno J, Fountain JJ, Martino CA, Reiley WW, Pearl JE, Winslow GM, Woodland DL, Randall TD & Cooper AM (2009) In a murine tuberculosis model, the absence of homeostatic chemokines delays granuloma formation and protective immunity. *J Immunol* 183: 8004–8014.

Kikuchi T, Matsuguchi T, Tsuboi N, Mitani A, Tanaka S, Matsuoka M, Yamamoto G, Hishikawa T, Noguchi T & Yoshikai Y (2001) Gene expression of osteoclast differentiation factor is induced by lipopolysaccharide in mouse osteoblasts via Toll-like receptors. *J Immunol* 166: 3574–3579.

Kim MS, Magno CL, Day CJ & Morrison NA (2006) Induction of chemokines and chemokine receptors CCR2b and CCR4 in authentic human osteoclasts differentiated with RANKL and osteoclast like cells differentiated by MCP-1 and RANTES. *J Cell Biochem* 97: 512–518.

Koizumi K, Saitoh Y, Minami T *et al.* (2009) Role of CX3CL1/fractalkine in osteoclast differentiation and bone resorption. *J Immunol* 183: 7825–7831.

Lam J, Abu-Amer Y, Nelson CA, Fremont DH, Ross FP & Teitelbaum SL (2002) Tumour necrosis factor superfamily cytokines and the pathogenesis of inflammatory osteolysis. *Ann Rheum Dis* 61(suppl 2): ii82–ii83.

Li X, Qin L, Bergenstock M, Bevelock LM, Novack DV & Partridge NC (2007) Parathyroid hormone stimulates osteoblastic expression of MCP-1 to recruit and increase the fusion of pre/osteoclasts. *J Biol Chem* 282: 33098–33106.

Mansell A, Brint E, Gould JA, O'Neill LA & Hertzog PJ (2004) Mal interacts with tumor necrosis factor receptor-associated factor (TRAF)-6 to mediate NF-kappaB activation by toll-like receptor (TLR)-2 and TLR4. *J Biol Chem* 279: 37227–37230.

Meghji S, White PA, Nair SP *et al.* (1997) *Mycobacterium tuberculosis* chaperonin 10 stimulates bone resorption: a potential contributory factor in Pott's disease. *J Exp Med* 186: 1241–1246.

Menu E, De Leenheer E, De Raeve H *et al.* (2006) Role of CCR1 and CCR5 in homing and growth of multiple myeloma and in the development of osteolytic lesions: a study in the 5TMM model. *Clin Exp Metastasis* 23: 291–300.

Oba Y, Lee JW, Ehrlich LA, Chung HY, Jelinek DF, Callander NS, Horuk R, Choi SJ & Roodman GD (2005) MIP-1alpha utilizes both CCR1 and CCR5 to induce osteoclast formation and increase adhesion of myeloma cells to marrow stromal cells. *Exp Hematol* 33: 272–278.

Okamoto M, Imaizumi K, Hasegawa Y, Hashimoto N, Sumida A, Shibazaki M, Takagi K, Shimokata K & Kawabe T (2007) Macrophage-derived chemokine in malignant and tuberculous pleural effusions. *Respirology* 12: 581–584.

Pathak SK, Basu S, Basu KK, Banerjee A, Pathak S, Bhattacharyya A, Kaisho T, Kundu M & Basu J (2007) Direct extracellular interaction between the early secreted antigen ESAT-6 of *Mycobacterium tuberculosis* and TLR2 inhibits TLR signaling in macrophages. *Nat Immunol* 8: 610–618.

Pethe K, Swenson DL, Alonso S, Anderson J, Wang C & Russell DG (2004) Isolation of *Mycobacterium tuberculosis* mutants defective in the arrest of phagosome maturation. *P Natl Acad Sci USA* 101: 13642–13647.

Pickens SR, Chamberlain ND, Volin MV, Pope RM, Mandelin AM 2nd & Shahrara S (2011) Characterization of CCL19 and CCL21 in rheumatoid arthritis. *Arthritis Rheum* 63: 914–922.

Ramakrishnan L (2012) Revisiting the role of the granuloma in tuberculosis. *Nat Rev Immunol* 12: 352–366.

Rohde K, Yates RM, Purdy GE & Russell DG (2007a) *Mycobacterium tuberculosis* and the environment within the phagosome. *Immunol Rev* 219: 37–54.

Rohde KH, Abramovitch RB & Russell DG (2007b) *Mycobacterium tuberculosis* invasion of macrophages: linking bacterial gene expression to environmental cues. *Cell Host Microbe* 2: 352–364.

Saitoh Y, Koizumi K, Sakurai H, Minami T & Saiki I (2007) RANKL-induced down-regulation of CX3CR1 via PI3K/Akt signaling pathway suppresses Fractalkine/CX3CL1-induced cellular responses in RAW264.7 cells. *Biochem Biophys Res Commun* 364: 417–422.

Schluger NW & Rom WN (1998) The host immune response to tuberculosis. *Am J Respir Crit Care Med* 157: 679–691.

Schmutz C, Cartwright A, Williams H, Haworth O, Williams JH, Filer A, Salmon M, Buckley CD & Middleton J (2010) Monocytes/macrophages express chemokine receptor CCR9 in rheumatoid arthritis and CCL25 stimulates their differentiation. *Arthritis Res Ther* 12: R161.

Stamm LM, Morisaki JH, Gao LY, Jeng RL, McDonald KL, Roth R, Takeshita S, Heuser J, Welch MD & Brown EJ (2003) *Mycobacterium marinum* escapes from phagosomes and is propelled by actin-based motility. *J Exp Med* 198: 1361–1368.

Suda K, Woo JT, Takami M, Sexton PM & Nagai K (2002) Lipopolysaccharide supports survival and fusion of preosteoclasts independent of TNF-alpha, IL-1, and RANKL. *J Cell Physiol* 190: 101–108.

Takami M, Kim N, Rho J & Choi Y (2002) Stimulation by toll-like receptors inhibits osteoclast differentiation. *J Immunol* 169: 1516–1523.

Takayanagi H, Iizuka H, Juji T, Nakagawa T, Yamamoto A, Miyazaki T, Koshihara Y, Oda H, Nakamura K & Tanaka S (2000a) Involvement of receptor activator of nuclear factor kappaB ligand/osteoclast differentiation factor in osteoclastogenesis from synoviocytes in rheumatoid arthritis. *Arthritis Rheum* 43: 259–269.

Takayanagi H, Ogasawara K, Hida S *et al.* (2000b) T-cell-mediated regulation of osteoclastogenesis by signalling cross-talk between RANKL and IFN-gamma. *Nature* 408: 600–605.

Takeda K & Akira S (2005) Toll-like receptors in innate immunity. *Int Immunol* 17: 1–14.

van der Wel N, Hava D, Houben D, Fluitsma D, van Zon M, Pierson J, Brenner M & Peters PJ (2007) *M. tuberculosis* and *M. leprae* translocate from the phagolysosome to the cytosol in myeloid cells. *Cell* 129: 1287–1298.

Volkman HE, Pozos TC, Zheng J, Davis JM, Rawls JF & Ramakrishnan L (2010) Tuberculous granuloma induction via interaction of a bacterial secreted protein with host epithelium. *Science* 327: 466–469.

Volpe E, Cappelli G, Grassi M, Martino A, Serafino A, Colizzi V, Sanarico N & Mariani F (2006) Gene expression profiling of human macrophages at late time of infection with *Mycobacterium tuberculosis*. *Immunology* 118: 449–460.

Welin A & Lerm M (2012) Inside or outside the phagosome? The controversy of the intracellular localization of *Mycobacterium tuberculosis*. *Tuberculosis (Edinb)* 92: 113–120.

WHO (2013) Tuberculosis Fact sheet No. 104. Media Centre, World Health Organization, http://www.who.int/tb/publications/factsheets/en/.

Wu C, Zhou Q, Qin XJ, Qin SM & Shi HZ (2010) CCL22 is involved in the recruitment of CD4+CD25 high T cells into tuberculous pleural effusions. *Respirology* 15: 522–529.

Yamada H, Mizuno S, Reza-Gholizadeh M & Sugawara I (2001) Relative importance of NF-kappaB p50 in mycobacterial infection. *Infect Immun* 69: 7100–7105.

Yamada H, Mizuno S & Sugawara I (2002) Interferon regulatory factor 1 in mycobacterial infection. *Microbiol Immunol* 46: 751–760.

Supporting Information

Additional Supporting Information may be found in the online version of this article:

Fig. S1. The expression levels of chemokine ligands by *Mtb*–infected monocytes, pre-osteoclasts, and multinuclear osteoclasts.

Fig. S2. The expression levels of chemokine receptors by monocytes, pre-osteoclasts, and multinuclear osteoclasts after *Mtb* stimulation.

JCM
Journals.ASM.org

Simple Multiplex PCR Assay for Identification of Beijing Family *Mycobacterium tuberculosis* Isolates with a Lineage-Specific Mutation in *Rv0679c*

Chie Nakajima,[a] Aki Tamaru,[b] Zeaur Rahim,[c] Ajay Poudel,[a] Bhagwan Maharjan,[d] Khin Saw Aye,[e] Hong Ling,[f] Toshio Hattori,[g] Tomotada Iwamoto,[h] Yukari Fukushima,[a] Haruka Suzuki,[a] Yasuhiko Suzuki,[a,i] Takashi Matsuba[j]

Division of Global Epidemiology, Hokkaido University Research Center for Zoonosis Control, Sapporo, Hokkaido, Japan[a]; Osaka Prefectural Institute of Public Health, Osaka, Japan[b]; Tuberculosis Laboratory, International Centre for Diarrhoeal Disease Research, Bangladesh, Dhaka, Bangladesh[c]; German Nepal Tuberculosis Project (GENETUP), Kathmandu, Nepal[d]; Immunology Research Division, Department of Medical Research (Lower Myanmar), Ministry of Health, Yangon, Myanmar[e]; Department of Microbiology, Harbin Medical University, Harbin, China[f]; Laboratory of Disaster-Related Infectious Diseases, International Research Institute of Disaster Sciences, Tohoku University, Sendai, Japan[g]; Department of Microbiology, Kobe Institute of Health, Kobe, Japan[h]; JICA/JST, SATREPS, Tokyo, Japan[i]; Division of Bacteriology, Department of Microbiology and Immunology, Faculty of Medicine, Tottori University, Yonago, Tottori, Japan[j]

The Beijing genotype of *Mycobacterium tuberculosis* is known to be a worldwide epidemic clade. It is suggested to be a possibly resistant clone against BCG vaccination and is also suggested to be highly pathogenic and prone to becoming drug resistant. Thus, monitoring the prevalence of this lineage seems to be important for the proper control of tuberculosis. The Rv0679c protein of *M. tuberculosis* has been predicted to be one of the outer membrane proteins and is suggested to contribute to host cell invasion. Here, we conducted a sequence analysis of the *Rv0679c* gene using clinical isolates and found that a single nucleotide polymorphism, C to G at position 426, can be observed only in the isolates that are identified as members of the Beijing genotype family. Here, we developed a simple multiplex PCR assay to detect this point mutation and applied it to 619 clinical isolates. The method successfully distinguished Beijing lineage clones from non-Beijing strains with 100% accuracy. This simple, quick, and cost-effective multiplex PCR assay can be used for a survey or for monitoring the prevalence of Beijing genotype *M. tuberculosis* strains.

The *Mycobacterium tuberculosis* Beijing genotype, first identified by van Soolingen et al. (1), is known to be a worldwide epidemic clade (2–4). Its possible resistance to BCG vaccination, in addition to its tendency to have a multidrug-resistant (MDR) phenotype, might give a selective advantage to the wide geographic distribution of the Beijing genotype strains (3, 5–7). Although some of the Beijing genotype strains show hypervirulence in animal infection models (7–9), neither the virulence factor nor the phenotypically specific factor of this lineage has been elucidated. The origin of the Beijing lineage is thought to be east Asia, where the prevalence of this clade is from around 40% to >90% (1, 3, 4, 10–13). However, in some other global areas, i.e., countries in the former Soviet Union and South Africa, the prevalence of the Beijing lineage has increased markedly in a short period, and some increases were suggested to be related to MDR (4, 11, 14). In those areas, higher clonality of the circulating strains was suggested, and most were categorized as being in the modern or typical Beijing clade, which is defined as a strain having one or two IS*6110* insertions in the noise transfer function (NTF) chromosomal region (11, 15). On the other hand, a higher variety of strains can be observed in east Asian countries. Especially in Japan and Korea, the majority of the strains belong to another cluster called the ancient or atypical Beijing clade (12, 16). Details regarding the higher pathogenicity of the Beijing lineage are controversial. Some studies have suggested that the modern Beijing clade is more prone to be pathogenic, tends to be drug resistant, and is likely able to escape from BCG vaccination (4, 8, 11, 14); however, some of the ancient Beijing clones were also shown to have higher pathogenicity (17) or a tendency toward acquiring drug resistance (16).

Since Beijing lineage prevalence has a great impact on the tuberculosis (TB) control program, several methods to distinguish this clade have been developed. First, van Soolingen et al. (1) identified this clade by its specific IS*6110* restriction fragment length polymorphism (RFLP) signatures. Soon after, these strains were shown to have a specific spoligotype pattern lacking spacer numbers 1 to 34, and this has been proposed as the definition of the clade (18, 19), since IS*6110* RFLP genotyping is time-consuming, and comparing results between laboratories is difficult. The deletion of spacers observed in the Beijing spoligotype is caused by the insertion of IS*6110* in the direct repeat (DR) region (18). Since this typical spoligotype pattern has become a specific marker of the Beijing genotype, some PCR methods to detect this specific deletion, named region of difference 207 (RD207), have been developed (20–22). In addition to RD207, another deleted region named RD105 was also shown to be a good marker for discrimination of the Beijing genotype, although this deletion is common for all the east Asian lineages, including the non-Beijing strains (10, 23); however, most of these published detection methods require expensive real-time PCR equipment and high-cost reagents (24). The conventional PCR assay targeting RD207 still seems to be at a disadvantage, since it relies on an unstable inser-

Received 23 December 2012 Returned for modification 11 February 2013
Accepted 4 April 2013
Published ahead of print 17 April 2013
Address correspondence to Takashi Matsuba, matsubat@med.tottori-u.ac.jp, or Yasuhiko Suzuki, suzuki@czc.hokudai.ac.jp.

doi:10.1128/JCM.03404-12

tion sequence that is likely to be a target of homologous recombination.

Instead of unstable repetitive structures, single nucleotide polymorphisms (SNPs) were recently considered to be a robust target for defining the accurate position of a strain on the phylogenetic tree, since horizontal gene transfer or gene recombination between different strains is rare in the *M. tuberculosis* complex (MTC) (12, 24, 25). Filliol et al. (26) drew phylogenetic trees of the MTC using several typing methods and showed that the dendrogram drawn with SNPs most accurately reflected the true evolution of the MTC. Some of those SNPs are suggested to be specific to the Beijing or east Asian lineages. In a search for membrane proteins that are suitable for vaccine antigens and/or are targets for the specific detection of the MTC, we found a candidate protein encoded by the *Rv0679c* gene. This protein was expressed on the cell surface as a lipoarabinomannan-associated protein (27, 28), and the coding sequence has an SNP that seems to be specific to the Beijing clade. In this study, we confirmed the lineage specificity of this SNP and developed a simple and low-cost multiplex PCR assay to distinguish the Beijing lineage strains.

MATERIALS AND METHODS

Preparation of genomic DNA from *M. tuberculosis* isolates. *M. tuberculosis* was isolated from the sputa or other clinical specimens of patients by conventional procedures using *N*-acetyl-L-cysteine (NALC)–NaOH. A total of 619 isolates obtained in Japan (n = 145), Bangladesh (n = 122), Nepal (n = 110), Myanmar (n = 198), and China (Heilongjiang Province, n = 44) were used in this study. Some of these isolates were the same as those in previous studies, and the details are described elsewhere (13, 29–31). Colonies grown on egg-based medium (either Ogawa or Löwenstein-Jensen medium) were resuspended in distilled water and boiled for 20 min, and the supernatant was used in the Bangladeshi and Myanmar samples. In the Japanese and Nepalese samples, colonies were suspended in 0.5 ml of 10 mM Tris-HCl, 1 mM EDTA (Tris-EDTA [TE] buffer [pH 8]), and 0.5 ml chloroform; 0.5 g glass beads of 0.17-mm diameter was added; and they were disrupted with a bead beater (MicroSmash; Tomy Seiko Co. Ltd., Tokyo, Japan). After centrifugation at 10,000 × *g* for 5 min, DNA in the supernatant was precipitated by ethanol, and the precipitated genomic DNA was resuspended in TE buffer for further use. In China, bacteria grown in a BACTEC *Mycobacterium* growth indicator tube (MGIT) (Becton, Dickinson and Company, Franklin Lakes, NJ) were used, and DNA was extracted by lysozymes and the phenol-chloroform method (13). All the DNA samples extracted in each country were brought to Japan, and the following steps were carried out in the Hokkaido University Research Center for Zoonosis Control. To determine the specificity of the method, DNAs extracted from five reference MTC strains (i.e., *M. tuberculosis* H37Rv, *Mycobacterium africanum* ATCC 25420, *Mycobacterium orygis* Z0001, *Mycobacterium microti* TC 89, and *Mycobacterium bovis* BCG Tokyo 172) and 30 nontuberculous mycobacterial (NTM) species, including *Mycobacterium avium*, *Mycobacterium intracellulare*, and *Mycobacterium kansasii*, were used.

Gene sequencing and comparison. A subset of 197 *M. tuberculosis* samples, 68 from Japan, 92 from Bangladesh, and 37 from Nepal, were chosen from the total 619 clinical isolates, and the *Rv0679c* gene fragment was amplified by PCR. The PCR mixture contained GoTaq PCR buffer (Promega Co., Madison, WI), 0.2 mM each deoxynucleoside triphosphate (dNTP), 0.3 μM each primers og0001 and og0002 (Table 1), 0.5 M betaine, 1 ng genomic DNA from *M. tuberculosis*, and 0.5 units of GoTaq polymerase. Amplification was carried out by applying 35 cycles of denaturation at 95°C for 10 s, annealing at 57°C for 10 s, polymerase reaction mixture at 72°C for 40 s, and a final extension at 72°C for 5 min. The amplified DNA fragment was subjected to sequence analysis with BigDye Terminator v3.1 (Life Technologies Co., Carlsbad, CA) reagents by a sequencer, the 3130 genetic analyzer (Life Technologies Co.), according to the manufacturer's protocol. The *Rv0679c* sequence was also compared with those of 80 whole-genome sequenced MTC strains registered in the GenBank (http://www.ncbi.nlm.nih.gov/GenBank/) or TB (http://genome.tbdb.org/annotation/genome/tbdb/MultiHome.html) (32) databases by the BLASTn algorithm (http://blast.ncbi.nlm.nih.gov/).

Genotyping. The spoligotype of *M. tuberculosis* clinical isolates was determined as described previously (33). Briefly, the DR region was amplified with a primer pair, and the PCR products were hybridized to a set of 43 spacer-specific oligonucleotide probes, which were covalently bound to the membrane. The spoligo-international type (SIT) was determined by comparing spoligotypes against the international spoligotyping database (SpolDB4) (3).

The detection of an RD105 deletion was performed by multiplex PCR in Beijing clones and by conventional PCR in east Asian strains other than those of the Beijing type, since the deletion pattern is different between those two groups (10). The reaction mixture consisted of GoTaq PCR buffer (Promega), 0.2 mM each dNTP, 0.3 μM (each) two or three primers (Table 1), 0.5 M betaine, 1 μl extracted DNA sample, and 0.5 units of GoTaq polymerase. The target was amplified by 35 cycles of denaturation at 95°C for 10 s, annealing at 55°C for 10 s, and extension at 72°C for 40 s, with a final extension at 72°C for 5 min. RD207 deletion was detected by two PCR assays described by Warren et al. (22), and TbD1 was detected by PCR using the Huard et al. (25) protocol (Table 1). The amplified DNA fragment was subjected to agarose gel electrophoresis with ethidium bromide (EtBr) to see the size of the band under a UV transilluminator.

The multilocus sequence type (MLST) was determined with 9 SNPs, which were described by Filliol et al. (26) and were selected for Beijing subtyping by Iwamoto et al. (16). Each locus was amplified with a primer pair (Table 1), and the product was subjected to sequencing. SNPs were detected by comparing the sequences with those of H37Rv (34). The sequence type (ST) was identified according to Filliol et al. (26).

Beijing lineage identification by multiplex PCR. Multiplex PCR for the identification of the Beijing lineage was performed under the following conditions. The PCR mixture, in a final volume of 15 μl, contained 1× PCR buffer (1.5 mM Mg; TaKaRa Bio, Inc., Shiga, Japan), 0.5 μl dNTP solution mix (10 mM each dNTP; New England BioLabs, Inc., Ipswich, MA), 0.5 μl each of Fw and R1 primers, 0.2 μl R2 primer (primer solutions in 10 μM; Table 1), 1.5 μl of 5 M betaine, 0.45 μl of 25 mM $MgCl_2$ (to make a final Mg concentration of 2.25 mM), 1 ng of sample DNA, and 0.5 units of TaKaRa Hot Start *Taq* polymerase (TaKaRa). Amplification was carried out with the first denaturation at 95°C for 1 min followed by 35 cycles of denaturation at 95°C for 10 s, annealing at 66°C for 10 s, extension at 72°C for 15 s, and the final extension at 72°C for 3 min. The amplicon was subjected to electrophoresis in a 2% agarose gel that included EtBr. DNA samples extracted from the isolate BCG Tokyo 172 and a well-characterized clinical isolate (Beijing OM-9) were used as controls for the non-Beijing and Beijing banding patterns, respectively. Sensitivity was determined with serially diluted genomic DNA obtained from these BCG and Beijing control strains. A specificity study was performed with genomic DNA samples (2 ng/μl each) from the MTC and NTM strains described above.

RESULTS

Spoligotyping and MLST. A total of 619 clinical isolates were subjected to spoligotyping, and 393 were identified as being in the Beijing lineage and 226 as a non-Beijing group (Table 2). The non-Beijing group consisted of a variety of strains belonging to the following lineages: east African-Indian (EAI), central Asian (CAS), Latin American Mediterranean (LAM), Haarlem, S, T, X, and non-Beijing east Asian (3). Ninety-four of the Beijing isolates were subjected to MLST analysis and were subtyped into 8 sequence-type classes, namely, ST26, ST3, STK, ST25, ST19, ST10, ST22, and ST8, which are listed in evolutional order from ancient to modern Beijing types (16, 26).

TABLE 1 Primers used in the study

Target	Primer name	Nucleotide sequence	Purpose	Reference
Rv0679c	og0001	CCGGGAACTAGGAATGGTAA	Sequencing	This study
	og0002	AGCAACCTCGCAATCTGAC	Sequencing	This study
	ON-1002 (Fw)	GTCACTGAACGTGGCCGGCTC	Multiplex PCR for Beijing type identification	This study
	ON-1258 (R1)[a]	TCGGTCACCGTTTTTGTAGGTGACCGTC	Multiplex PCR for Beijing type identification	This study
	ON-1127 (R2)	AGCAACCTCGCAATCTGACC	Multiplex PCR for Beijing type identification	This study
RD105	RD105-F (−239~−218)	GGAAAGCAACATACACACCACG	Multiplex PCR for east Asian type determination[b]	This study
	RD105-R	AGGCCGCATAGTCACGGTCG	Multiplex PCR for east Asian type determination[b]	This study
	RD105-M (+304~323)	TCCTGGGTGCCGAACAAGTG	Multiplex PCR for east Asian type determination[b]	This study
	RD105EA-F (−80~−60)	TCGGACCCGATGGCTTCGGTG	PCR for east Asian type determination[c]	This study
	RD105EA-R (61~42)	TGATCACGGTTCGCCCGCAG	PCR for east Asian type determination[c]	This study
RD207	RD207-1F (Warren)	TTCAACCATCGCCGCCTCTAC	PCR for Beijing type identification (set 1)	22
	RD207-1R (Warren)	CACCCTCTACTCTGCGCTTTG	PCR for Beijing type identification (set 1)	22
	RD207-2F (Warren)	ACCGAGCTGATCAAACCCG	PCR for Beijing type identification (set 2)	22
	RD207-2R (Warren)	ATGGCACGGCCGACCTGAATGAACC	PCR for Beijing type identification (set 2)	22
TbD1	TbD1F	CGTTCAACCCCAAACAGGTA	PCR for ancestral *M. tuberculosis* determination	25
	TbD1R	AATCGAACTCGTGGAACACC	PCR for ancestral *M. tuberculosis* determination	25
797736[d]	Beijing ST-1F	GACGGCCGAATCTGACACTG	MLST for Beijing lineage	This study
	Beijing ST-1R	CCATTCCGGGTGGTCACTG	MLST for Beijing lineage	This study
909164[d]	Beijing ST-2F	CGTCGAGCTCCCACTTCTTG	MLST for Beijing lineage	This study
	Beijing ST-2R	TCGTCGAAGTGGACGAGGAC	MLST for Beijing lineage	This study
1477596[d]	Beijing ST-3F	GTCGACAGCGCCAGAAAATG	MLST for Beijing lineage	This study
	Beijing ST-3R	GCTCCTATGCCACCCAGCAC	MLST for Beijing lineage	This study
1692067[d]	Beijing ST-5F	GATTGGCAACTGGCAACAGG	MLST for Beijing lineage	This study
	Beijing ST-5R	TGGCCGTTTCAGATAGCACAC	MLST for Beijing lineage	This study
1892015[d]	Beijing ST-6F	GCTGCACATCATGGGTTGG	MLST for Beijing lineage	This study
	Beijing ST-6R	GTATCGAGGCCGACGAAAGG	MLST for Beijing lineage	This study
2376133[d]	Beijing ST-7F	TCTTGCGACCCGATGTGAAC	MLST for Beijing lineage	This study
	Beijing ST-7R	GAGCGCAACATGGGTGAGTC	MLST for Beijing lineage	This study
2532614[d]	Beijing ST-8F	CCCTTTTCTGCTCGGACACG	MLST for Beijing lineage	This study
	Beijing ST-8R	GATCGACCTTCGTGCACTGG	MLST for Beijing lineage	This study
2825579[d]	Beijing ST-9F	CCTTGGAGCGCAACAAGATG	MLST for Beijing lineage	This study
	Beijing ST-9R	CTGGCCGGACGATTTTGAAG	MLST for Beijing lineage	This study
4137829[d]	Beijing ST-10F	CGTCGCTGCAATTGTCTGG	MLST for Beijing lineage	This study
	Beijing ST-10R	GGACGCAGTCGCAACAGTTC	MLST for Beijing lineage	This study

[a] Beijing-type specific mutation-detection primer. Underlined 2-base sequences at the 5′ end are not complementary sequences.
[b] This assay was used for Beijing genotype strains.
[c] This assay was used for non-Beijing genotype strains.
[d] This SNP nucleotide position on the *H37Rv* genome is according to references 26 and 34.

Sequence analysis of the *Rv0679c* gene of *M. tuberculosis* isolates. Nucleotide sequences of the full-length *Rv0679c* gene obtained from 197 clinical *M. tuberculosis* isolates collected in Japan, Bangladesh, and Nepal were compared with the *Rv0679c* sequence in *M. tuberculosis* H37Rv (34). Only a single nucleotide difference of cytosine to guanine at position 426, which leads to an amino acid change at codon 142 from Asn (AAC) to Lys (AAG), was detected in 87 isolates, all of which were identified as being in the Beijing lineage by spoligotyping and, supportively, by RD207 PCR (22) (data not shown). One Bangladeshi isolate showed a mixed peak of C and G at position 426 and was revealed as a mixed culture of Beijing and another strain by RD105 and RD207 detection PCR (Table 2). None of the non-Beijing isolates had the mutation, and vice versa. In public databases, 14 strains reported from several countries were revealed to have this mutation, and all were confirmed as being in the Beijing lineage by checking for the RD207 deletion *in silico* (18). None of the other 66 MTC strains, which were determined to be non-Beijing, had this mutation. The 498-bp *Rv0679c* sequence was well conserved among the MTC strains, and the following three strains in the database showed alterations: *M. tuberculosis* strains C and T17 and *Mycobacterium canettii* CIPT 140010059.

TABLE 2 *Rv0679c* multiplex PCR results compared with other typing results in 619 *M. tuberculosis* clinical isolates

Isolate origin	Spoligotype family[a]	RD207, RD105, or other typing methods[b]	Sequence type[c]	*Rv0679c* M-PCR type[d]	No. of isolates
Beijing or Beijing-like					393
Japan	Beijing	ND	26	Beijing	10
	Beijing	ND	3	Beijing	24
	Beijing	ND	STK	Beijing	13
	Beijing-like	RD207$^+$	STK	Beijing	1
	Beijing	ND	25	Beijing	3
	Beijing	ND	19	Beijing	9
	Beijing	ND	10	Beijing	12
	Beijing	ND	22	Beijing	4
	Beijing	ND	ND	Beijing	23
Bangladesh	Beijing	ND	26	Beijing	3
	Beijing	ND	10	Beijing	12
	Beijing	ND	22	Beijing	2
	Beijing	ND	8	Beijing	1
	Beijing	ND	ND	Beijing	29
	Beijing-like	RD105$^+$, RD207$^+$	ND	Beijing	1
Nepal	Beijing	ND	ND	Beijing	64
Myanmar	Beijing	ND	ND	Beijing	141
	Beijing-like	RD105$^+$, RD207$^+$	ND	Beijing	1
China (Heilongjiang)	Beijing	ND	ND	Beijing	40
Non-Beijing or undesignated/new[a]					216
Japan	Undesignated/new[e]	RD105$^+$, RD207$^-$	ND	Non-Beijing	29
	Others[f]	ND	ND	Non-Beijing	16
Bangladesh	—[g]	ND	ND	Non-Beijing	73
Nepal	—[h]	ND	ND	Non-Beijing	45
Myanmar	—[i]	ND	ND	Non-Beijing	51
China (Heilongjiang)	Undesignated/new	ND	ND	Non-Beijing	2
Mixed clone samples					6
Bangladesh	Undesignated/new	Mixed peak in sequence[j] RD105$^+$, RD207$^+$	ND	Beijing	1
Myanmar	Undesignated/new	RD105$^+$, RD207$^+$	ND	Beijing	2
	EAI2_NTB	RD105$^+$	ND	Beijing	1
	EAI5	RD105$^+$	ND	Beijing	1
China (Heilongjiang)	Undesignated/new	RD105$^+$	ND	Beijing	1
New spoligotype lacking spacers 1–34[k]					4
Japan	New	RD105$^+$, RD207$^+$[k]	ND	Beijing	1
Nepal	New	RD105$^-$, TbD1$^+$[k]	ND	Non-Beijing	1
Myanmar	New	RD105$^+$, RD207$^+$	ND	Beijing	1
China (Heilongjiang)	New	RD105$^+$, RD207$^+$	ND	Beijing	1

[a] Spoligotype labeling is according to SpolDB4 (3).
[b] A positive superscript indicates that a deletion was detected; a minus superscript indicates that the RD was not deleted or the region was intact. ND, not determined.
[c] Sequence type is according to reference 26.
[d] M-PCR, multiplex PCR.
[e] East Asian lineage.
[f] Including the clades LAM1, LAM9, T1, T2, T3, T3-Osaka, and new (other than the east Asian lineage).
[g] Including the clades EAI1_SOM, EAI2-MANILA, EAI3_IND, EAI5, EAI6_BGD1, EAI7_BGD2, EAI unidentified, CAS, CAS1-DHLHI, CAS2, LAM9, T1, T4, H1, H3, X1, X2, and undesignated/new.
[h] Including the clades EAI3_IND, EAI5, CAS, CAS1-DHLHI, LAM1, LAM5, T1, T2, T3, H3, S, and undesignated/new.
[i] Including the clades EAI2_MANILA, EAI2_NTB, EAI5, EAI6_BGD1, EAI7_BGD2, CAS1-DHLHI, LAM9, T1, T3, X2, S, and undesignated/new.
[j] Overlapped peak of C and G was observed at nucleic acid position 426.
[k] Details are described in Table 3.

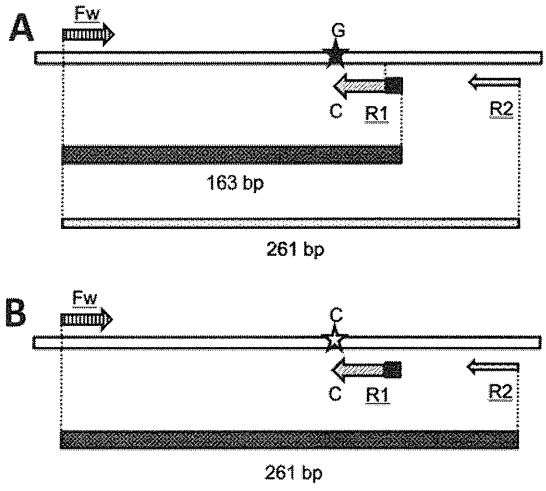

FIG 1 PCR primers and products of *Rv0679c*-targeting multiplex PCR for Beijing lineage discrimination. (A) In the Beijing sample, the 163-bp product is amplified more dominantly than is the 261-bp product. (B) In the non-Beijing sample, 163-bp product is not amplified because of the mismatch of the 3′ end of R1. Fw, forward primer; R1, reverse primer 1 (Beijing lineage specific); R2, reverse primer 2. Two-base noncomplement nucleotides at the 5′ end are shown by black squares.

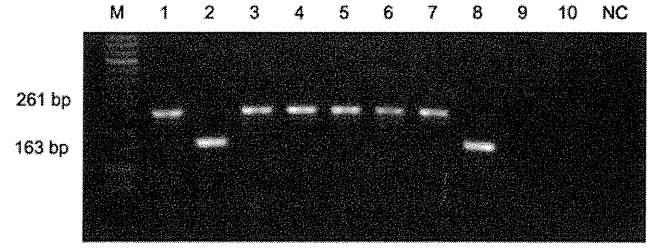

FIG 2 Electrophoresis results of the multiplex PCR products. Lane M, 50-bp ladder DNA size marker; lane 1, *M. bovis* BCG Tokyo 172 (non-Beijing lineage control) strain; lane 2, *M. tuberculosis* OM-9 strain (Beijing lineage control); lane 3, *M. tuberculosis* H37Rv; lane 4, *M. africanum* ATCC 25420; lanes 5–8, *M. tuberculosis* clinical isolates (lane 5, non-Beijing east Asian; lane 6, EAI; lane 7, LAM9; lane 8, Beijing); lane 9, *M. avium* strain JATA51-1; lane 10, *M. kansasii* JATA21-1; lane NC, negative control.

In strain C, the C185T SNP was observed, and in T17, a cytosine was inserted at position 92. In *M. canettii* CIPT 140010059, two SNPs and a codon insertion, ACC at position 154, were observed.

Beijing lineage identification by multiplex PCR. Multiplex PCR was developed targeting the Beijing-specific SNP on *Rv0679c*, employing a primer with the mutated nucleic acid at the 3′ end of the sequence (primer R1; Fig. 1 and Table 1); the optimal reaction conditions were determined as described in Materials and Methods. With this system, a bright band of 163 bp was observed as an amplified product of the primers Fw and R1 in the Beijing genotype samples (Fig. 1A and 2). An additional band of 261 bp, which is the product of primers Fw and R2, can be seen depending on the conditions, although it is always significantly thinner than the 163-bp band because of the low R2-primer concentration (see Materials and Methods). In contrast, only the 261-bp band is observed in a non-Beijing genotype sample (Fig. 1B and 2). Since the sequences of the primers are specific to the MTC, no amplification occurs in the absence of MTC genomic DNA (Fig. 2, data for *M. avium* and *M. kansasii*). A total of 619 clinical isolates obtained in the five Asian countries of Japan, Bangladesh, Nepal, Myanmar, and China were subjected to this Beijing lineage-identifying multiplex PCR, and the results were compared with their spoligotypes. All the isolates determined as having a Beijing or Beijing-like genotype by the SpolDB4 (n = 393) were determined to be in the Beijing lineage by the multiplex PCR (Table 2). On the other hand, no samples that included only non-Beijing genotype DNA (n = 216) were identified as being in the Beijing lineage. Twenty-nine non-Beijing east Asian lineage strains, which were suggested by a characteristic spoligotype having spacer 34 and were defined by RD105 detection, were determined to be non-Beijing by the multiplex PCR. Six isolates that showed a discrepancy between their spoligotype and the multiplex PCR result were further determined by RD207 or RD105 detection PCR and were revealed to be a mixture of Beijing and other subtype strains (mixed clone samples, Table 2). Four samples from different countries had confusing spoligotypes that lacked spacers 1 to 34 and additionally lacked some of the spacers from 35 to 43. These samples could also be identified correctly (Tables 2 and 3). The minimum detection limits were 100 and 1,000 cells per reaction in the Beijing genotype and BCG strains, respectively (data not shown).

DISCUSSION

In this study, we demonstrated that the SNP of C to G at position 426 in the *Rv0679c* gene is specific to the Beijing genotype strains. We developed a new multiplex PCR using this SNP to identify Beijing lineage isolates. This PCR assay successfully distinguished Beijing genotype strains from others, including the non-Beijing east Asian strains, with 100% accuracy. The Beijing lineage genotype is usually identified by spoligotyping, specific patterns of IS*6110* RFLP, or the detection of RD207, which is led by an insertion of IS*6110* in the DR region. However, spoligotyping is well known to show gene conversions, and strains having no genetic relationship sometimes show the same spoligotype (3, 26). Fenner et al. (35) reported pseudo-Beijing strains that had a typical Beijing spoligotype even though they actually belonged to the CAS family. This type of confusion seems to occur especially in areas that have a higher prevalence of principal genetic group 1 (PGG1) lineages, including the EAI, CAS, and east Asian lineages, since PGG1 strains usually possess spacers 35 and 36, which are lacking in PGG2 and PGG3 strains (3, 36). In other areas, mixed infections of more than two strains sometimes disrupt correct spoligotyping by showing mixed spacer patterns. The Manu1-SIT100 and Manu2-SIT54 types, which lack the spacers 34 or 33 and 34, respectively, are known to be producible by the mixture of Beijing family and T1 strains (3, 37). In this study, we found that some samples showed discrepant results between *Rv0679c* multiplex PCR and spoligotyping that determined a strain to be of the Beijing genotype by multiplex PCR, despite having another spoligotype. Using RD105 and RD207 detection methods, all of these samples were confirmed to be a mixture of Beijing and another strain. This type of mixed culture is sometimes observed in countries with a higher TB burden, where a coinfection of more than two strains is not rare (22). Some of the spoligopatterns of those samples showed faint positive spacers, suggesting the mixed presence of other strains. Even clear and correct spoligotypes can sometimes lead to misjudgments. In the current study, some samples showed only one to several spacers to be positive in the Beijing spacer area,

TABLE 3 Typing result comparison in clinical isolates having confusing spoligotype patterns

Sample (identification)	Spoligotype pattern	Spoligotype family[a]	*Rv0679c* M-PCR type	Detection type				Final typing result
				RD207 set 1[b]	RD207 set 2[b]	RD105	TbD1	
Japan (O-05-44)		New	Beijing	−	+[c]	+	−	Beijing
Nepal (no. 51)		New	Non-Beijing	−	−	−	+	Ancestral[d]
Myanmar (no. 95)		New	Beijing	+	+	+	ND	Beijing
China (2460)		New[e]	Beijing	+	+	+	ND	Beijing

[a] These patterns were not found in the SpolDB4 list.
[b] PCR sets 1 and 2 in reference 22.
[c] A faint correctly sized band and an additional band of a different size were observed.
[d] Ancestral type of *M. tuberculosis* strain possessing TbD1 region (25).
[e] The spoligotype pattern of this sample has been reported in reference 13.

namely, from spacers 35 to 43. Most were identified as being of the Beijing genotype by multiplex PCR, while one was judged to be a non-Beijing strain. All Beijing genotype-positive results were confirmed by RD105 and RD207 PCRs, and the non-Beijing isolate was revealed as an "ancestral type," which involves EAI but not the Beijing lineage, by TbD1 detection (Table 3) (25). These examples support the high specificity and applicability of this SNP-targeting PCR. The disadvantages of IS*6110* RFLP and RD207 detection have already been described above. RD207-detection PCR did not work as expected in the sample that lost spacers 1 to 42 (Japan O-05-44; Table 3), suggesting that some additional reconstruction had occurred at the IS*6110* insertion site of the DR region. SNPs in MTC genomes can provide robust lineage information, whereas repetitive elements, such as direct repeats in the DR region, the mycobacterial interspersed repetitive unit (MIRU) tandem repeats (38), or IS*6110*, are prone to alteration. One hundred percent concordance of the PCR results with the genetically confirmed Beijing type is not surprising because of the rigidity of the SNPs in the MTC (25, 26). Of the 393 Beijing family isolates, 94 were subtyped by MLST and consisted of 8 STs covering a wide range of the Beijing family, from ancient to modern types (Table 2). This suggested that a specific mutation in *Rv0679c* seemed to have occurred in the Beijing lineage at the same time as the RD207 deletion event.

Rv0679c is an MTC-specific gene, as shown by Cifuentes et al. (27), and no significantly similar sequence was detected by an NCBI BLASTn search in the GenBank database. Thus, this multiplex PCR assay can be used for the identification of the MTC, as well as for the differentiation of Beijing and non-Beijing lineages (Fig. 2). The Beijing mutation detection primer (R1; Fig. 1 and Table 1) was designed to have two additional noncomplement bases at the 5′ end to block the second amplification by the PCR product that produces the 261-bp fragment with an outer R2 primer. Additionally, the higher concentration and melting temperature of the R1 primer compared to those of the outer R2 primer increase the Fw-R1 product more than the Fw-R2 product. With these techniques, the Beijing band (163 bp) can be shown to be significantly brighter than the non-Beijing band (261 bp) when the sample is derived from Beijing lineage *M. tuberculosis* strains (Fig. 2). The relatively higher annealing temperature of 66°C gave good contrast of those two bands and prevented nonspecific amplifications. Modified *Taq* or other polymerases that have 3′-to-5′ exonuclease activity should be avoided, since those enzymes can trim the mutated nucleotide at the R1 primer end. It is recommended to check the PCR conditions using positive controls for Beijing and non-Beijing types (i.e., BCG) every time (Fig. 2). The detection limit of 100 to 1,000 copies per reaction might be relatively high; however, it can be improved by about 10 times by increasing the PCR cycle number to 40, although the necessity of identifying the MTC lineage in direct clinical specimens seems to be low.

In papers featuring SNPs as epidemiological markers, synonymous mutations are usually selected to avoid the effect of evolutional pressure (26). However, both SNPs for the differentiation of PGG1, PGG2, and PGG3 were nonsynonymous mutations in *katG* and *gyrA* (36), and so far, they have provided robust differentiation results. In the MTC, nonsynonymous mutations on functional genes can be observed in a relatively higher frequency than in other bacteria because of extremely reduced purifying selection pressure (39). Thus, nonsynonymous mutations can be preserved unless they are significantly disadvantageous. Indeed, 100% of the Beijing family strains in the current study could be identified with this nonsynonymous mutation, suggesting that it at least has no adverse effect on those strains. The function of the Rv0679c protein is still unclear, although its expression on the cell surface has been confirmed (27, 28). Cifuentes et al. (27) reported that the surface-localized Rv0679c protein contributed to the *M. tuberculosis* invasion of host cells and proposed the protein as a vaccine candidate. The substituted amino acid at position 142 was located in the C-terminus region of the protein, which was included in the "high-activity binding peptide" to target cells (27). Thus, this highly conserved nonsynonymous SNP, which results in an amino acid substitution with different characteristics (Asn → Lys), might have some biological meaning in explaining Beijing lineage pathogenicity. Since BCG vaccine strains, as well as other non-Beijing strains, have Rv0679c-Asn142, this substitution might affect the antigenicity of the Beijing bacterial surface and might contribute to the possible evasion of BCG-derived immunity. Further investigation of the association of the Rv0679c Asn142Lys substitution with Beijing strain outer membrane characteristics and antigenicity is ongoing.

In conclusion, a simple, robust, and low-cost multiplex PCR assay for the detection of Beijing lineage *M. tuberculosis* strains was successfully developed using a Beijing-specific SNP on *Rv0679c*. This PCR assay can be used in local laboratories to monitor the prevalence of the Beijing genotype, and this is strongly recommended to control this possibly highly pathogenic and drug resistance-prone sublineage.

ACKNOWLEDGMENTS

This work was supported in part by a grant from the U.S.-Japan Cooperative Medical Science Programs from the Ministry of Health, Labor, and Welfare of Japan (to Y.S.), by the Global Center of Excellence (COE) Program "Establishment of International Collaboration Centers for Zoonosis Control," Ministry of Education, Culture, Sports, Science, and Technology of Japan (MEXT) (to Y.S.), by the Japan Initiative for Global Research Network on Infectious Diseases (J-GRID) from MEXT (to Y.S.), and by a grant for the Joint Research Program of the Research Center for Zoonosis Control, Hokkaido University by MEXT (to Y.S., C.N., and T.M.), as well as by grants-in-aid for scientific research from the Japan Society for the Promotion of Science (JSPS) (to Y.S. and C.N.).

REFERENCES

1. **van Soolingen D, Qian L, de Haas PE, Douglas JT, Traore H, Portaels F, Qing HZ, Enkhsaikan D, Nymadawa P, van Embden JD.** 1995. Predominance of a single genotype of *Mycobacterium tuberculosis* in countries of east Asia. J. Clin. Microbiol. 33:3234–3238.
2. **Bifani PJ, Mathema B, Kurepina NE, Kreiswirth BN.** 2002. Global dissemination of the *Mycobacterium tuberculosis* W-Beijing family strains. Trends Microbiol. 10:45–52.
3. **Brudey K, Driscoll JR, Rigouts L, Prodinger WM, Gori A, Al-Hajoj SA, Allix C, Aristimuño L, Arora J, Baumanis V, Binder L, Cafrune P, Cataldi A, Cheong S, Diel R, Ellermeier C, Evans JT, Fauville-Dufaux M, Ferdinand S, Garcia de Viedma D, Garzelli C, Gazzola L, Gomes HM, Guttierez MC, Hawkey PM, van Helden PD, Kadival GV, Kreiswirth BN, Kremer K, Kubin M, Kulkarni SP, Liens B, Lillebaek T, Ho ML, Martin C, Martin C, Mokrousov I, Narvskaïa O, Ngeow YF, Naumann L, Niemann S, Parwati I, Rahim Z, Rasolofo-Razanamparany V, Rasolonavalona T, Rossetti ML, Rüsch-Gerdes S, Sajduda A, Samper S, Shemyakin IG, et al.** 2006. *Mycobacterium tuberculosis* complex genetic diversity: mining the fourth international spoligotyping database (SpolDB4) for classification, population genetics and epidemiology. BMC Microbiol. 6:23. doi:10.1186/1471-2180-6-23.
4. **Hanekom M, Gey van Pittius NC, McEvoy C, Victor TC, Van Helden PD, Warren RM.** 2011. *Mycobacterium tuberculosis* Beijing genotype: a template for success. Tuberculosis (Edinb.) 91:510–523.
5. **Colditz GA, Brewer TF, Berkey CS, Wilson ME, Burdick E, Fineberg HV, Mosteller F.** 1994. Efficacy of BCG vaccine in the prevention of tuberculosis. Meta-analysis of the published literature. JAMA 271:698–702.
6. **de Steenwinkel JE, ten Kate MT, de Knegt GJ, Kremer K, Aarnoutse RE, Boeree MJ, Verbrugh HA, van Soolingen D, Bakker-Woudenberg IAJM.** 2012. Drug susceptibility of *Mycobacterium tuberculosis* Beijing genotype and association with MDR TB. Emerg. Infect. Dis. 18:660–663.
7. **Parwati I, van Crevel R, van Soolingen D.** 2010. Possible underlying mechanisms for successful emergence of the *Mycobacterium tuberculosis* Beijing genotype strains. Lancet Infect. Dis. 10:103–111.
8. **López B, Aguilar D, Orozco H, Burger M, Espitia C, Ritacco V, Barrera L, Kremer K, Hernandez-Pando R, Huygen K, van Soolingen D.** 2003. A marked difference in pathogenesis and immune response induced by different *Mycobacterium tuberculosis* genotypes. Clin. Exp. Immunol. 133:30–37.
9. **Reed MB, Domenech P, Manca C, Su H, Barczak AK, Kreiswirth BN, Kaplan G, Barry CE, III.** 2004. A glycolipid of hypervirulent tuberculosis strains that inhibits the innate immune response. Nature 431:84–87.
10. **Chuang PC, Chen HY, Jou R.** 2010. Single-nucleotide polymorphism in the *fadD28* gene as a genetic marker for east Asia lineage *Mycobacterium tuberculosis*. J. Clin. Microbiol. 48:4245–4247.
11. **Mokrousov I, Ly HM, Otten T, Lan NN, Vyshnevskyi B, Hoffner S, Narvskaya O.** 2005. Origin and primary dispersal of the *Mycobacterium tuberculosis* Beijing genotype: clues from human phylogeography. Genome Res. 15:1357–1364.
12. **Wada T, Iwamoto T, Maeda S.** 2009. Genetic diversity of the *Mycobacterium tuberculosis* Beijing family in east Asia revealed through refined population structure analysis. FEMS Microbiol. Lett. 291:35–43.
13. **Wang J, Liu Y, Zhang CL, Ji BY, Zhang LZ, Shao YZ, Jiang SL, Suzuki Y, Nakajima C, Fan CL, Ma YP, Tian GW, Hattori T, Ling H.** 2011. Genotypes and characteristics of clustering and drug susceptibility of *Mycobacterium tuberculosis* isolates collected in Heilongjiang Province, China. J. Clin. Microbiol. 49:1354–1362.
14. **Cowley D, Govender D, February B, Wolfe M, Steyn L, Evans J, Wilkinson RJ, Nicol MP.** 2008. Recent and rapid emergence of W-Beijing strains of *Mycobacterium tuberculosis* in Cape Town, South Africa. Clin. Infect. Dis. 47:1252–1259.
15. **Plikaytis BB, Marden JL, Crawford JT, Woodley CL, Butler WR, Shinnick TM.** 1994. Multiplex PCR assay specific for the multidrug-resistant strain W of *Mycobacterium tuberculosis*. J. Clin. Microbiol. 32:1542–1546.
16. **Iwamoto T, Yoshida S, Suzuki K, Wada T.** 2008. Population structure analysis of the *Mycobacterium tuberculosis* Beijing family indicates an association between certain sublineages and multidrug resistance. Antimicrob. Agents Chemother. 52:3805–3809.
17. **Kato-Maeda M, Shanley CA, Ackart D, Jarlsberg LG, Shang S, Obregon-Henao A, Harton M, Basaraba RJ, Henao-Tamayo M, Barrozo JC, Rose J, Kawamura LM, Coscolla M, Fofanov VY, Koshinsky H, Gagneux S, Hopewell PC, Ordway DJ, Orme IM.** 2012. Beijing sublineages of *Mycobacterium tuberculosis* differ in pathogenicity in the guinea pig. Clin. Vaccine Immunol. 19:1227–1237.
18. **Beggs ML, Eisenach KD, Cave MD.** 2000. Mapping of *IS6110* insertion sites in two epidemic strains of *Mycobacterium tuberculosis*. J. Clin. Microbiol. 38:2923–2928.
19. **Kremer K, Glynn JR, Lillebaek T, Niemann S, Kurepina NE, Kreiswirth BN, Bifani PJ, van Soolingen D.** 2004. Definition of the Beijing/W lineage of *Mycobacterium tuberculosis* on the basis of genetic markers. J. Clin. Microbiol. 42:4040–4049.
20. **Hillemann D, Warren R, Kubica T, Rüsch-Gerdes S, Niemann S.** 2006. Rapid detection of *Mycobacterium tuberculosis* Beijing genotype strains by real-time PCR. J. Clin. Microbiol. 44:302–306.
21. **Sun JR, Lee SY, Dou HY, Lu JJ.** 2009. Using a multiplex polymerase chain reaction for the identification of Beijing strains of *Mycobacterium tuberculosis*. Eur. J. Clin. Microbiol. Infect. Dis. 28:105–107.
22. **Warren RM, Victor TC, Streicher EM, Richardson M, Beyers N, Gey van Pittius NC, van Helden PD.** 2004. Patients with active tuberculosis often have different strains in the same sputum specimen. Am. J. Respir. Crit. Care Med. 169:610–614.
23. **Tsolaki AG, Gagneux S, Pym AS, Goguet de la Salmoniere YOL, Kreiswirth BN, Van Soolingen D, Small PM.** 2005. Genomic deletions classify the Beijing/W strains as a distinct genetic lineage of *Mycobacterium tuberculosis*. J. Clin. Microbiol. 43:3185–3191.
24. **Stucki D, Malla B, Hostettler S, Huna T, Feldmann J, Yeboah-Manu D, Borrell S, Fenner L, Comas I, Coscollà M, Gagneux S.** 2012. Two new rapid SNP-typing methods for classifying *Mycobacterium tuberculosis* complex into the main phylogenetic lineages. PLoS One 7:e41253. doi:10.1371/journal.pone.0041253.
25. **Huard RC, Fabre M, de Haas P, Lazzarini LC, van Soolingen D, Cousins D, Ho JL.** 2006. Novel genetic polymorphisms that further delineate the phylogeny of the *Mycobacterium tuberculosis* complex. J. Bacteriol. 188:4271–4287.
26. **Filliol I, Motiwala AS, Cavatore M, Qi W, Hazbón MH, Bobadilla del Valle M, Fyfe J, García-García L, Rastogi N, Sola C, Zozio T, Guerrero MI, León CI, Crabtree J, Angiuoli S, Eisenach KD, Durmaz R, Joloba ML, Rendón A, Sifuentes-Osornio J, Ponce de León A, Cave MD, Fleischmann R, Whittam TS, Alland D.** 2006. Global phylogeny of *Mycobacterium tuberculosis* based on single nucleotide polymorphism (SNP) analysis: insights into tuberculosis evolution, phylogenetic accuracy of other DNA fingerprinting systems, and recommendations for a minimal standard SNP set. J. Bacteriol. 188:759–772.
27. **Cifuentes DP, Ocampo M, Curtidor H, Vanegas M, Forero M, Patarroyo ME, Patarroyo MA.** 2010. *Mycobacterium tuberculosis* Rv0679c protein sequences involved in host-cell infection: potential TB vaccine candidate antigen. BMC Microbiol. 10:109. doi:10.1186/1471-2180-10-109.
28. **Matsuba T, Suzuki Y, Tanaka Y.** 2007. Association of the Rv0679c protein with lipids and carbohydrates in *Mycobacterium tuberculosis*/*Mycobacterium bovis* BCG. Arch. Microbiol. 187:297–311.
29. **Poudel A, Nakajima C, Fukushima Y, Suzuki H, Pandey BD, Maharjan B, Suzuki Y.** 2012. Molecular characterization of multidrug-resistant *Mycobacterium tuberculosis* isolated in Nepal. Antimicrob. Agents Chemother. 56:2831–2836.
30. **Rahim Z, Nakajima C, Raqib R, Zaman K, Endtz HP, van der Zanden AG, Suzuki Y.** 2012. Molecular mechanism of rifampicin and isoniazid resistance in *Mycobacterium tuberculosis* from Bangladesh. Tuberculosis (Edinb.) 92:529–534.
31. **Tamaru A, Nakajima C, Wada T, Wang Y, Inoue M, Kawahara R, Maekura R, Ozeki Y, Ogura H, Kobayashi K, Suzuki Y, Matsumoto S.**

2012. Dominant incidence of multidrug and extensively drug-resistant specific *Mycobacterium tuberculosis* clones in Osaka Prefecture, Japan. PLoS One 7:e42505. doi:10.1371/journal.pone.0042505.

32. **Reddy TB, Riley R, Wymore F, Montgomery P, DeCaprio D, Engels R, Gellesch M, Hubble J, Jen D, Jin H, Koehrsen M, Larson L, Mao M, Nitzberg M, Sisk P, Stolte C, Weiner B, White J, Zachariah ZK, Sherlock G, Galagan JE, Ball CA, Schoolnik GK.** 2009. TB database: an integrated platform for tuberculosis research. Nucleic Acids Res. 37(Database issue):D499–D508. doi:10.1093/nar/gkn652.
33. **Kamerbeek J, Schouls L, Kolk L, van Agterveld M, van Soolingen D, Kuijper S, Bunschoten A, Molhuizen H, Shaw R, Goyal M, van Embden J.** 1997. Simultaneous detection and strain differentiation of *Mycobacterium tuberculosis* for diagnosis and epidemiology. J. Clin. Microbiol. 35: 907–914.
34. **Cole ST, Brosch R, Parkhill J, Garnier T, Churcher C, Harris D, Gordon SV, Eiglmeier K, Gas S, Barry CE, III, Tekaia F, Badcock K, Basham D, Brown D, Chillingworth T, Connor R, Davies R, Devlin K, Feltwell T, Gentles S, Hamlin N, Holroyd S, Hornsby T, Jagels K, Krogh A, McLean J, Moule S, Murphy L, Oliver K, Osborne J, Quail MA, Rajandream MA, Rogers J, Rutter S, Seeger K, Skelton J, Squares R, Squares S, Sulston JE, Taylor K, Whitehead S, Barrell BG.** 1998. Deciphering the biology of *Mycobacterium tuberculosis* from the complete genome sequence. Nature 393:537–544.
35. **Fenner L, Malla B, Ninet B, Dubuis O, Stucki D, Borrell S, Huna T, Bodmer T, Egger M, Gagneux S.** 2011. "Pseudo-Beijing": evidence for convergent evolution in the direct repeat region of *Mycobacterium tuberculosis*. PLoS One 6:e24737. doi:10.1371/journal.pone.0024737.
36. **Sreevatsan S, Pan X, Stockbauer KE, Connell ND, Kreiswirth BN, Whittam TS, Musser JM.** 1997. Restricted structural gene polymorphism in the *Mycobacterium tuberculosis* complex indicates evolutionarily recent global dissemination. Proc. Natl. Acad. Sci. U. S. A. 94:9869–9874.
37. **Lazzarini LC, Rosenfeld J, Huard RC, Hill V, Lapa e Silva JR, DeSalle R, Rastogi N, Ho JL.** 2012. *Mycobacterium tuberculosis* spoligotypes that may derive from mixed strain infections are revealed by a novel computational approach. Infect. Genet. Evol. 12:798–806.
38. **Supply P, Mazars E, Lesjean S, Vincent V, Gicquel B, Locht C.** 2000. Variable human minisatellite-like regions in the *Mycobacterium tuberculosis* genome. Mol. Microbiol. 36:762–771.
39. **Hershberg R, Lipatov M, Small PM, Sheffer H, Niemann S, Homolka S, Roach JC, Kremer K, Petrov DA, Feldman MW, Gagneux S.** 2008. High functional diversity in *Mycobacterium tuberculosis* driven by genetic drift and human demography. PLoS Biol. 6:e311. doi:10.1371/journal.pbio.0060311.

Infection, Genetics and Evolution 21 (2014) 479–483

Contents lists available at ScienceDirect

Infection, Genetics and Evolution

journal homepage: www.elsevier.com/locate/meegid

Intra-subspecies sequence variability of the MACPPE12 gene in *Mycobacterium avium* subsp. *hominissuis*

Tomotada Iwamoto [a,*], Kentaro Arikawa [a], Chie Nakajima [b], Noriko Nakanishi [a], Yukiko Nishiuchi [c], Shiomi Yoshida [d], Aki Tamaru [e], Yutaka Tamura [f], Yoshihiko Hoshino [g], Heekyung Yoo [h], Young Kil Park [h], Hajime Saito [i], Yasuhiko Suzuki [b]

[a] Department of Infectious Diseases, Kobe Institute of Health, 4-6 Minatojima-nakamachi, Chuo-ku, Kobe 650-0046, Japan
[b] Division of Global Epidemiology, Hokkaido University Research Center for Zoonosis Control, Kita-20, Nishi-10, Kita-ku, Sapporo 001-0020, Japan
[c] Toneyama Institute for Tuberculosis Research, Osaka City University Medical School, Osaka 560-8552, Japan
[d] Clinical Research Center, National Hospital Organization Kinki-chuo Chest Medical Center, 1180 Nagasone-cho, Sakai, Osaka 591-8555, Japan
[e] Department of Bacteriology, Osaka Prefectural Institute of Public Health, 3-69, Nakamichi 1-chome, Higashinari-ku, Osaka 537-0025, Japan
[f] School of Veterinary Medicine, Rakuno Gakuen University, 583 Midorimachi Bunkodai, Ebetsu, Hokkaido 069-8501, Japan
[g] Leprosy Research Center, National Institute of Infectious Diseases, Tokyo 189-0002, Japan
[h] Research and Development, Korean Institute of Tuberculosis, Korean National Tuberculosis Association, 482, Mansu-ri, Kangwoi-myun, Cheongwon-gun, Chungbuk 363-954, South Korea
[i] Yoshijima Hospital, 2-33, Yoshijima-higashi 3 chome, Naka-ku, Hiroshima 730-0822, Japan

ARTICLE INFO

Article history:
Received 10 June 2013
Received in revised form 11 August 2013
Accepted 12 August 2013
Available online 20 September 2013

Keywords:
Mycobacterium avium subsp. *hominissuis*
PE/PPE gene family
Variable numbers of tandem repeats
SNPs
Genetic diversity

ABSTRACT

The PE (Pro-Glu) and PPE (Pro-Pro-Glu) multigene families are unique to mycobacteria, and are highly expanded in the pathogenic members of this genus. We determined the intra-subspecies genetic variability of the MACPPE12 gene, which is a specific PPE gene in *Mycobacterium avium* subsp. *hominissuis* (MAH), using 334 MAH isolates obtained from different isolation sources (222 human isolates, 145 Japanese and 77 Korean; 37 bathroom isolates; and 75 pig isolates). In total, 31 single-nucleotide polymorphisms (SNPs), which consisted of 16 synonymous SNPs and 15 nonsynonymous SNPs, were determined through comparison with the MACPPE12 gene sequence of MAH strain 104 as a reference. As the result, the 334 MAH isolates were classified into 19 and 13 different sequevars at the nucleic acid level (NA types) and amino acid level (AA types), respectively. Among the 13 AA types, only one type, the AA02 type, presented various NA types (7 different types) with synonymous SNPs, whereas all other AA types had a one-to-one correspondence with the NA types. This finding suggests that AA02 is a longer discernible lineage than the other AA types. Therefore, AA02 was classified as an ancestral type of the MACPPE12 gene, whereas the other AA types were classified as modern types. The ubiquitous presence of AA02 in all of the isolation sources and all different sequevars classified by the *hsp65* genotype further supports this classification. In contrast to the ancestral type, the modern types showed remarkable differences in distribution between human isolates and pig isolates, and between Japanese isolates and Korean isolates. Divergence of the MACPPE12 gene may thus be a good indicator to characterize MAH strains in certain areas and/or hosts.

1. Introduction

Mycobacterial infections caused by strains of the *Mycobacterium avium* complex (MAC) are becoming increasingly prevalent in animals and humans (Falkinham, 2010; Turenne et al., 2006; Winthrop, 2010). In particular, *Mycobacterium avium* subsp. *hominissuis* (MAH) is a frequent agent of human and pig mycobacteriosis (Mijs et al., 2002). Although MAH is typically considered to be an opportunistic bacterium for immunocompromised persons, it also frequently occurs in immunocompetent individuals and generally manifests as a slowly progressive, often debilitating lung disease. Recently, middle-aged and elderly females without any predisposing conditions have been suggested to bear the brunt of this disease (Inagaki et al., 2009). Therefore, it has been speculated that MAH-associated mycobacteriosis is caused not only by host characteristics but also by bacterial factors (Ichikawa et al., 2009).

The PE (Pro-Glu) and PPE (Pro-Pro-Glu) multigene families are unique to mycobacteria and are suspected to be involved in immunostimulation and virulence (Gey van Pittius et al., 2006; Mackenzie et al., 2009; Sampson, 2011). The PE and PPE gene families are highly expanded in the pathogenic species of this genus (Gey van Pittius et al., 2006). Recently, Mackenzie et al., 2009 identified 12 PE and 49 PPE orthologs in the major groups of the MAC; *Mycobac-*

* Corresponding author. Tel.: +81 78 302 6251; fax: +81 78 302 0894.
E-mail address: tomotada_iwamoto@office.city.kobe.lg.jp (T. Iwamoto).

1567-1348/$ - see front matter © 2013 Elsevier B.V. All rights reserved.
http://dx.doi.org/10.1016/j.meegid.2013.08.010

terium avium subsp. *paratuberculosis*, *M. avium* subsp. *hominissuis*, *Mycobacterium avium* subsp. *avium*, and *Mycobacterium intracellulare*. A genomic comparison among them identified the subspecies-specific PE/PPE genes and the missing PE/PPE genes from one subspecies but present in at least two members of the MAC (Mackenzie et al., 2009). The former are likely to emerge and/or be acquired after divergence into the certain subspecies, whereas the latter are likely to correspond to earlier deletions in the certain subspecies. Two PPE genes, i.e., Mav 0790c and Mav 2006, which are now denoted as MACPPE4 and MACPPE12, respectively, under the newly proposed uniform PE and PPE locus names for all members of the MAC, were specific for MAH strain 104. The corresponding gene products could be used to identify immune responses against this *M. avium* subspecies, and misinterpretations caused by cross-reactivity in current diagnostics for Johne's disease would thus be avoided (Mackenzie et al., 2009).

In this study, we first confirmed that MACPPE12 is ubiquitous in this subspecies, whereas MACPPE4 is not widely distributed in strains other than MAH strain 104. To determine the intra-subspecies genetic variations of the MACPPE12 gene, we sequenced the full length of the gene (1341 bp) using 334 isolates that were obtained from different sources, i.e., 222 human isolates (145 Japanese and 77 Korean), 37 bathroom isolates, and 75 pig isolates. We also determined whether the genetic variation was associated with the isolation source.

2. Material and methods

2.1. Bacterial isolates

We used crude DNA extracted from 334 isolates for this study. Of these isolates, 257 overlapped with 258 isolates that were previously identified as MAH by *hsp65* sequencing analyses and used to analyze genetic diversity (Iwamoto et al., 2012). One isolate from our previous study bank was excluded because of a lack of volume. We newly added 77 isolates from 77 human patients that were obtained from 7 different cities in Korea between 2010 and 2011. They were originally identified as *M. avium* through sequencing of the 16S rRNA gene (Devulder et al., 2005) at the Korean Institute of Tuberculosis. The *hsp65* sequencing analyses that were performed in this study confirmed that all of the isolates belonged to MAH. To compare the genetic diversity of the 77 MAH isolates with the previously obtained data for the other 257 isolates, the same genetic markers used in the previous study (Iwamoto et al., 2012), i.e., the 3′ portion of the *hsp65* gene sequence, presence of IS*Mav6*, and genotypes of the 19-locus variable number of tandem repeat (VNTR) sequence, were analyzed for the 77 isolates. The datasets used in this study consisted solely of sequence data and no personal data were disclosed at any point.

2.2. PCR and sequencing of MACPPE12

The MACPPE12 gene, the locus name of which in MAH strain 104 (accession number in GenBank, NC_008595) is Mav_2006, was amplified using the primer sets MAV2006F (5′-TGC GTG GTA ACA AAA GCA AC) and MAV2006R (5′-CTT GCT GCG TAA TGC GAT AA). The PCR reaction consisted of 94 °C for 3 min followed by 30 cycles of 94 °C for 1 min, 55 °C for 1 min, and 72 °C for 1 min, with a final extension at 72 °C for 7 min. PCR was performed using Ex Taq Hot Start Version (TaKaRa Bio Inc., Shiga, Japan) with GC buffer I (TaKaRa Bio Inc., Shiga, Japan), and the PCR products were subjected to sequence analysis using an AB3500 genetic analyzer system (Applied Biosystems, Foster City, CA). The same primers used for PCR were also used for the sequencing of forward and reverse fragments. In addition, the interim primers MAV2006F634 (AAC GCG CTG CAG AAT CTC) and MAV2006R824 (TCC GTC ATC TTG TGT TCA GC) were used for the sequencing of forward and reverse fragments, respectively. Detailed information regarding VNTR genotypes, *hsp65* code types, presence of IS*Mav6*, and MACPPE12 sequevars of the 334 isolates in this study are summarized in Supplemental Table 1 (Table S1).

2.3. Phylogenetic analysis

The split-network phylogeny of the complete MACPPE12 gene sequence (1341 bp) was computed by NeighborNet analysis in SplitTree Version 4.8 (Huson and Kloepper, 2005). Recombination events in the MACPPE12 gene within the 334-isolate set were evaluated using DnaSP 4.10 (Rozas et al., 2003).

2.4. Nucleotide accession numbers

Sequences of the complete MACPPE12 gene representing each sequevar recognized in this study (NA types 2 to 19) were deposited in GenBank under accession Nos. AB820302 to AB820319.

3. Results

3.1. Presence of MACPPE4 and MACPPE12 in MAH

In a preliminary study, we first evaluated the ubiquitous presence of two previously reported MAH-specific MACPPE genes, i.e., MACPPE4 and MACPPE12, in MAH by using 16 randomly selected MAH isolates obtained from humans ($n = 6$), bathroom samples ($n = 2$), and pigs ($n = 8$). We attempted to detect the MACPPE4 gene using two PCR primer sets, one targeting the outside regions of MACPPE4, which can amplify the whole MACPPE4 gene with its flanking region, and the other targeting the inside sequences of MACPPE4, which can amplify partial regions of the gene. These primer sets produced expected sizes of PCR products from MAH strain 104 but the amplicons were not obtained from 16 other strains (data not shown). We therefore assumed that the MACPPE4 gene is not universally present in this subspecies, MAH. On the other hand, MACPPE12 was detected from all of the 16 isolates using the primer set targeting the outside regions of the gene, which can amplify whole MACPPE12 gene with its flanking region. Our expanding analysis for all of 334 samples could detect MACPPE12 from all of them. Therefore, it is highly likely that MACPPE12 is a ubiquitous gene in MAH.

3.2. Sequence variation of the MACPPE12 gene

First, we assured our sample set consisted of reasonably high heterogeneous isolates for the evaluation of the genetic variability and distribution of the MACPPE12 gene in MAH by 19-locus VNTR analysis. Actually, we retrieved the data from our previous study (Iwamoto et al., 2012) for 257 isolates and added newly analyzed data for 77 Korean isolates. The data demonstrated a reasonably high degree of genetic diversity in this sample set (Table 1 and Table S1). In brief, 99 genotypes in 145 Japanese isolates, 49 genotypes in 77 Korean isolates, 27 genotypes in 37 bathroom isolates, and 38 genotypes in 75 pig isolates.

The sequence analysis of the full length of the MACPPE12 gene for 334 MAH isolates identified in total 31 SNPs, which formed 19 different MACPPE12 sequevars at the nucleic acid (NA) level (NA type) through comparison with the MACPPE12 gene sequence of MAH strain 104 as a reference (Table 1). Of the 31 SNP positions, 15 positions were nonsynonymous SNPs (nsSNPs) that caused amino acid substitutions. This relatively high ratio of nsSNPs resulted in the formation of 13 different sequevars at the amino acid (AA)

Table 1
SNPs among the *M. avium* subsp. *hominissuis* in comparison with prototype strain *M. avium* subsp. *hominissuis* strain 104 (MAH strain 104).

Amino acid type	Nucleic acid type	Nucleotide at the base pair position of strain MAH strain 104[a]																							Total number of:[b]			
		4*	66	88*	272*	468	558	571*	605*	715*	733	744	752*	765	822	829*	831	834	866*	867	868*	870	877*	924	978	1000	1005	1150*	1161	1163*	1192*	1330*	sSNP	nsSNP	Isolates (n = 334)	Genotypes
AA01	NA01	C	A	G	A	T	T	G	C	C	C	G	G	G	A	C	G	T	G	G	G	C	G	G	G	G	A			31		12
AA02	NA02	C	A	G	A	T	T	G	C	C	C	G	G	G	A	C	G	T	G	G	G	C	G	G	G	G	G	0	1	130		86
AA02	NA03	C	A	G	A	C	T	G	C	C	T	G	G	G	A	C	G	T	G	G	G	C	G	G	G	G	G	2	1	8		6
AA02	NA04	C	A	G	A	C	T	G	C	C	C	G	G	G	A	C	G	T	G	G	G	C	G	G	G	G	G	1	1	3		3
AA02	NA05	C	G	G	A	C	T	G	C	C	C	G	G	G	A	C	G	T	G	G	G	C	G	G	G	G	G	2	1	2		2
AA02	NA06	C	G	G	A	T	T	G	C	C	C	G	G	G	A	C	G	T	G	G	G	C	G	G	G	G	G	1	1	1		1
AA02	NA07	C	A	G	A	T	T	G	C	C	C	G	G	G	A	C	G	T	G	G	G	C	G	T	G	G	G	1	1	1		1
AA02	NA08	C	A	G	A	C	C	G	C	C	C	G	G	G	A	C	G	T	G	G	G	C	G	C	G	G	G	2	1	1		1
AA03	NA09	C	G	A	A	T	C	G	C	C	C	G	G	G	G	T	C	T	G	G	G	C	C	C	G	G	G	5	4	89		44
AA04	NA10	C	A	G	A	T	T	G	T	C	C	G	G	G	A	C	G	T	G	G	G	C	G	C	G	G	G	0	2	7		6
AA05	NA11	C	A	G	A	T	T	G	C	C	C	G	G	G	A	C	G	T	G	G	G	C	G	C	A	A	A	G	1	3	1		1
AA06	NA12	C	G	A	A	T	C	G	C	C	C	G	G	G	A	C	G	T	G	G	G	C	G	C	G	G	G	2	2	1		1
AA07	NA13	C	G	G	A	C	C	G	C	C	C	G	G	G	G	T	G	T	G	G	A	C	G	C	G	G	G	5	2	19		14
AA08	NA14	C	A	G	G	C	C	G	C	C	C	G	G	G	G	T	G	T	G	G	G	C	T	A	C	G	G	5	4	19		9
AA09	NA15	T	A	G	A	T	C	G	C	C	C	G	G	T	G	T	G	T	G	G	G	C	C	C	G	G	G	3	4	10		5
AA10	NA16	C	G	A	A	T	C	G	C	C	C	G	T	G	G	G	T	C	T	G	G	C	C	A	G	G	G	5	5	3		3
AA11	NA17	C	A	G	A	T	T	A	C	T	C	G	G	G	A	C	G	T	G	G	G	C	G	C	G	G	G	0	3	1		1
AA12	NA18	C	G	A	A	T	C	G	C	C	C	G	G	G	T	G	T	G	T	G	G	C	G	C	G	G	G	3	3	1		1
AA13	NA19	C	A	G	A	C	C	G	C	C	C	A	G	A	A	G	T	G	A	A	G	C	G	C	G	G	A	7	4	6		3

[a] Asterisks denote nonsynonymous position. AA01 and NA01 is the sequevars for MAH strain 104.
[b] sSNP, synonimous SNP; nsSNP, nonsynonymous SNP; genotypes were defined by 19-VNTR.

level (AA types) (Table 1). Among the 13 AA types, only AA02 showed variation in the nucleic acid sequence, i.e., it matched seven different NA types (NA02 to 08) that possessed various synonymous SNPs (sSNPs) (Table 1). All other AA types were associated in a one-to-one correspondence with NA types. These results suggest that AA02 has a longer history than the other AA types in MAH. We, therefore, classified AA02 as the ancestral type of MACPPE 12, whereas the other AA types were classified as modern types. When we used DnaSP, the minimum number of recombination events for the MACPPE12 gene in the sample set was estimated to be 3. The unrooted phylogeny for the gene sequences determined by SplitsTree4 demonstrated complex web-like topology (Fig. 1).

3.3. Comparison of the divergence of MACPPE12 in different isolation sources

The ancestral AA type of MACPPE12, AA02, was observed in all of the different isolation sources in this study (Table 2). In contrast, the modern types varied according to the isolation source. AA01 and AA07-09 were mostly present in pigs; AA03, in Japanese humans and bathroom samples; and AA13, in Korean humans. The topological positions of these AA types in the unrooted tree, except for that of AA01, were distinct from the position of the ancestral type (AA02) (Fig. 1).When we compared variation of MACPPE12 AA types with that of the *hsp65* gene sequevar, which consists of only sSNPs in this sample set, the AA02 type was observed in all 11 *hsp65* code types (Table 2). This would be natural due to the ancestral feature of AA02. Apart from the ancestral type, most of the modern types were distributed across more than two *hsp65* code types and not in a single lineage. This data strongly suggested that these two genes diverged independently, not in parallel to each other, during the history of MAH. It would be noteworthy that 57 pig isolates with *hsp65* code type 1, which was characterized as predominant code type of pig isolates in our previous study (Iwamoto et al., 2012), were subclassified into 5 AA types: AA01 ($n = 26$), AA02 ($n = 4$), AA07 ($n = 12$), AA08 ($n = 11$), and AA09 ($n = 4$) (Table 2, and Table S1).

A further finding in this study is the commonality and differences between Japanese and Korean human clinical isolates. A high prevalence of IS*Mav6*, which was reported in the genetic characterization of MAH in Japan (Ichikawa et al., 2009), was also observed in Korean isolates (42/77, 54.5%) as was reported by (Niimi et al., 2012). The characteristics of Korean isolates was demonstrated by their high prevalence of *hsp65* sequevar code 16 (26/77, 33.8%), which is a rare sequevar in other countries (Ichikawa et al., 2009; Iwamoto et al., 2012; Turenne et al., 2006). The majority of Korean isolates were ancestral type (AA02), whereas Japanese isolates predominated both AA02 and AA03. Moreover, other modern AA types showed different distributions between samples from these two countries.

4. Discussion

The precise functions of the PE and PPE families are still unknown except for a certain small number of members (Karboul et al., 2008; Mishra et al., 2008; Sassetti and Rubin, 2003), but these families are highly suspected to play key roles in the interaction between pathogens and their host (habitat) (Brennan et al., 2001; Sampson, 2011). A recent comparative study (Mackenzie et al., 2009) of the whole genomes of different MAC organisms revealed that two PPE paralogs, MACPPE4 and MACPPE12, were specifically found in MAH strain 104. Therefore, it would be a reasonable assumption that the two PPE genes reflect bacteriological characteristics of MAH in comparison with other MAC species.

Table 2
Characterization of MACPPE12 gene sequevars according to *hsp65* gene sequence and source of the 334 isolates.

MAC PPE 12		*hsp65* Code Type											Source			
AA type	NA type	C1	C2	C3	C7	C9	C15	C16	C17	N1	N2	N3	Human (Japan)	Human (Korea)	Bath-room	Pig
AA01	NA01	26	4	1	–	–	–	–	–	–	–	–	3	–	–	28
AA02	NA02-08	9	68	2	4	3	21	32	2	1	3	1	72	57	12	5
AA03	NA09	1	21	–	–	1	59	2	5	–	–	–	57	10	22	–
AA04	NA10	–	3	–	–	–	3	–	1	–	–	–	5	–	2	–
AA05	NA11	–	–	–	–	–	1	–		–	–	–	1	–	–	–
AA06	NA12	–	–	–	–	–	–	–	1	–	–	–	1	–	–	–
AA07	NA13	13	5	–	–	–	–	–	1	–	–	–	2	–	–	17
AA08	NA14	11	5	–	–	1	1	1	–	–	–	–	4	–	–	15
AA09	NA15	4	2	–	–	–	–	–	1	3	–	–	–	–	–	10
AA10	NA16	–	1	–	–	–	2	–	–	–	–	–	–	2	1	–
AA11	NA17	–	–	–	–	–	–	1	–	–	–	–	–	1	–	–
AA12	NA18	–	–	–	–	–	–	–	–	–	1	–	–	1	–	–
AA13	NA19	–	–	6	–	–	–	–	–	–	–	–	–	6	–	–

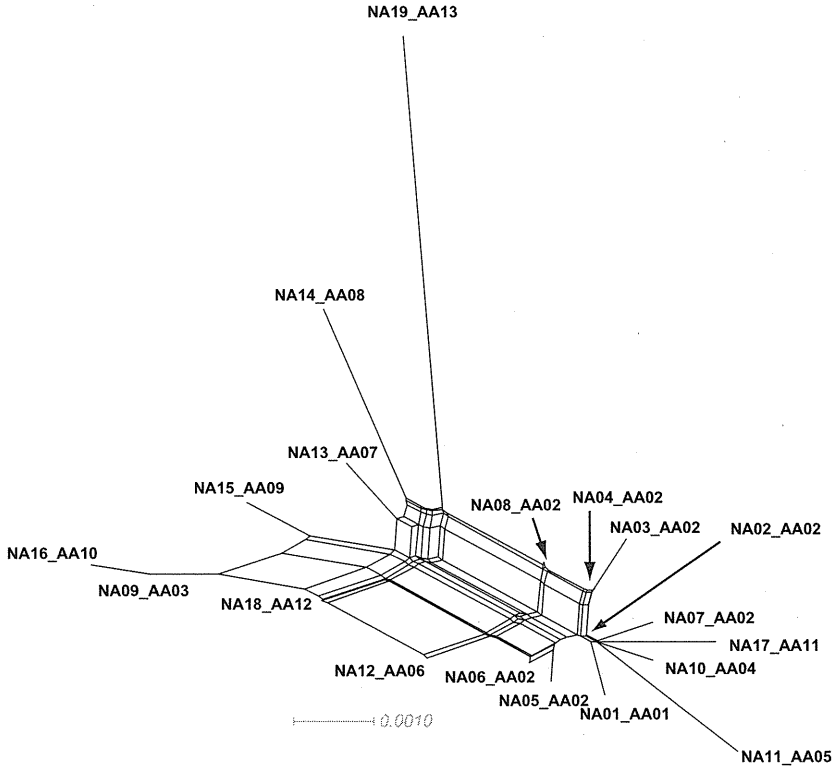

Fig. 1. Phylogenetic representation of each AA and NA type determined in this study and generated in SplitsTree4.

In this study, we evaluated the ubiquitous presence of these two PPE genes in MAH, and their genetic variability and association with the isolation sources and different genetic markers.

Our preliminary study using 16 MAH isolates suggested that MACPPE4 is not ubiquitous in MAH, although it is not certain that if this PPE gene is specific only for MAH strain104 or limited in subgroups of MAH. On the other hand, MACPPE12 was present in all of the 334 MAH isolates. Since our 334 isolates were a set of high heterogeneous isolates, the ubiquitous presence of the PPE gene in this sample set strongly supports the idea that this gene was present in the most recent common ancestor of MAH and universally retained in the subspecies. Because of the absence of the MACPPE12 gene in other members of the MAC and the ubiquitous presence in MAH isolates, MACPPE12 can be considered as a relatively new gene but ubiquitous in MAH.

By using the large number of isolates obtained from different sources, we demonstrated the variability of MACPPE12, which includes 19 different NA types and 13 AA types (Table 1). The web-like topology of the unrooted phylogeny (Fig. 1) and the estimated minimum number of recombination events suggest that genetic recombination plays a role in the divergence of this gene, although its mechanism is unknown. On the basis of the distribution of SNPs, isolation sources, and *hsp65* code types in the different MACPPE12 gene AA types, we classified the PPE gene into two groups; one is an ancestral type (AA02) and the other is a modern type. MAH is generally characterized as its ubiquitous host distribution and heterogeneous grouping (Turenne et al., 2008, 2007). However, when we look closely at the correlation between AA types and isolation sources, the distribution of the modern AA types well reflect their isolation sources, whereas the ancestral AA type (AA02) was observed in all of the different isolation sources. Thus, it can be hypothesized that emergence of the modern AA types somehow reflects an on-going evolution of MAH toward specialization (narrower range for host specificity and higher fitness to its habitat)